International Journal of Applied Engineering Research ISSN 0973-4562 Volume 10, Number 15 (2015) pp 35971-35991


# Experimental And Numerical Investigation On Flow Induced Vibration Excitation In Engineering Structures: A Review

**K.Karthik Selva Kumar***
Senior Research Fellow,
Department of Mining Machinery Engineering,
Indian School of Mines, Dhanbad,
Jharkhand, India
kksk88@gmail.com

**L.A.Kumaraswamidhas,**
Associate Professor,
Department of Mining Machinery Engineering,
Indian School of Mines, Dhanbad,
Jharkhand, India
lakdhas1978@gmail.com

Abstract- In this paper an attempt has been made to systematically organize the research investigations of experimental, analytical/numerical approach on flow induced vibration in the Engineering Structures, so far. Before presenting the experimental, analytical and numerical approach, an introduction about the behavior of flow induced vibration in various fields of engineering, is discussed. The literature review on the experimental approach of various researchers was categorized under the different subdivisions such as wind tunnel facility, arrangement of bluff bodies, flow motion/direction and the dimensionless parameters. Review on the research work performed by employing different numerical approach were categorized as, ALE formulation, LES and the LBM. In the conclusion, the results of various researchers are analyzed and finally the suggestion for the suppression of flow induced vibration in bluff bodies is discussed.

Keywords: Flow Induced Vibration, Computational Fluid Dynamics, Turbulence, and Vortex Shedding.

## Introduction

When the bluff bodies are exposed to a steady and uniform flow, an interaction between the fluid and the structures will take place resulting into a fluctuating pressure force of considerable magnitude causing the Flow Induced Vibrations. Nowadays, the studies on the Flow Induced Vibration (FIV) have drastically increased in various fields of engineering and non-engineering applications. The vibrations induced by the fluid flow can be classified according to the nature of the fluid structure interaction, as shown in the following table.1 In this paper it was symmetrically organized the research investigation of flow induced vibration on the bluff bodies, particularly the studies on the fluid flow past the bluff bodies in the aspect of engineering. The fluid-flows are broadly classified into internal, external and free shear flow. The present study is about the FIV due to the external flow of fluid over the bluff bodies i.e. circular, square or the rectangular cylinders. Basically interaction between the fluids and the structures were more complex phenomena to study. D. Shiels et al, (2001) found out that the FIV of an elastically constrained 2-D circular cylinder has become a significant problem in studying the interaction between the fluids and structures. For these type of problem L. Cheng, Y. Zhou (2008), suggested the novel surface perturbation technique to control fluid–structure interactions, including vortex streets, flow-induced vibrations and vortex-induced noise. From the view of various researchers, some possible sources for the FIV and its analyzing techniques are stated below.

TABLE.1. Mechanism causing Vibration by the Nature of Fluid Structure Interaction. (K.Karthik Selva Kumar & L.A.Kumaraswamidhas (2014))

| MECHANISM CAUSING VIBRATION | | | |
|---|---|---|---|
| 1. | Additional added masses | 8. | Galloping and flutter |
| 2. | Inertial coupling effect | 9. | Induced vibration due to fluid elastic instability |
| 3. | Instability due to parallel flow | 10. | Multi-phase buffeting |
| 4. | Induced vibration due to turbulence | 11. | Acoustic resonance |
| 5. | Induced vibration due to ocean wave | 12. | Hydraulic transients |
| 6. | Sonic fatigue | 13. | Environmental excitation |
| 7. | Induced vibration due to vortex shedding | 14. | Transmitted mechanical vibration |

The FIV can be developed due to an alternating low-pressure, caused by the vortex shedding, behind a submerged cylinder, Hyun-Boo Lee, et al (2013). From the studies of M.J. Pettigrew et al (1998), it was identified that the occurrences of vibration induced in the tube bundles by the cross flow, is mainly due to the fluid elastic instability. Ajith Kumar, R. and Gowda, B.H.L (2006), Korkischko, I., and Meneghini, J.R (2010) suggested that the total number of cylinders and its arrangements was one of the parameters which has significant impact on the induced vibration due to fluid flow. H.S. Kang et al., (2003), proposed an axial-flow-induced vibration model to evaluate the sensitivity to spring stiffness on the FIV of the bluff bodies. The important parameters of the heat exchangers to withstand the FIV are damping, mass per unit length, mass ratio, etc. which must be significantly evaluated at the stage of designing, H. Gelbe et al, (1995). Biswas and Ahamed, (2001), investigated the self-excited lateral vibration of a pipe due to an internal fluid flow and

applied an integral minimum principle of Pontryagin, to find the optimum flow velocity for minimum pipe vibration (i.e. to maximize the fluid transport efficiency), it is necessary to maximize the flow velocity while minimizing the lateral vibration of the pipe. L. Perotin and S. Granger, (1998), predicted that the dynamic behavior of the tube equipped with all the linear and non-linear supports, deduced from an identified turbulent excitation, provides a highly satisfactory validation for the regularized inverse identification process. Sang-Nyung Kim, and Yeon-Sik Cho, (2004), applied a mode frequency analysis, subroutine of Structural Routine in ANSYS, to carry out the analysis of the natural frequency and relative amplitude of the tube. B.A. Jubran et al., (1998), applied the newly developed joint time-frequency analysis techniques (JTFA) and in particular, the modulated Gaussian wavelet to identify the characteristics of the FIV of an elastically mounted single cylinder subjected to the cross flow. Kumar, R.A. et al., (2008) analyzed the flow-induced oscillations of a square section cylinder under interference conditions using a data-mining tool called 'decision tree'. Using numerical and experimental analysis K.Karthik Selva Kumar & L.A.K Dhas (2014 & 2015) investigated the vibration excitation behavior of circular and square section at different orientation. Wu, W. et al., (2007), investigated the high-frequency perturbation effects on the performance, to suppress the FIV in the bluff bodies.. The component failures due to excessive FIV, continue to affect the performance and reliability of the equipment's; such failures are very costly in terms of repairs which lead to loss of the production, Pettigrew, M.J., et al (1998). To suppress the FIV in the bluff bodies, many of the researchers have done a lot of experimental work in different aspects which were as follows

In recent years, numerous studies on the FIV in the bluff bodies, especially in the circular cylinders were carried out in different phenomenon such as, the vortex shedding of stationary bluff body to the vortex shedding of an elastic body. The vortices generated due to the flow over the bluff bodies, resulted in the induced vibration which depend on various factors such as the vortex shedding frequency, Reynolds numbers, correlation of the force components, the material damping, the structural stiffness of the cylinder and the added mass effect. In this chapter, the summarization of experimental work which was conducted by many researchers so far, has been described. For the different gap ratios Sarvghad-Moghaddam., et al, (2011), analyzed and calculated the pressure field, the vorticity distribution along with the associated streamlines and the time histories of hydrodynamic forces. While R.A. Kumar et al. (2008) performed an experimental analysis for various size ratios of test cylinder with the interfering cylinder values of 0.5, 1.0, 1.5 and 2.0, respectively. For a rigid cylinder G.R. Franzini et al., (2009), experimentally investigated, by mounting the bluff bodies on a low damping elastic base which was inclined in relation to the vertical, by an angle $\theta$ of $20^{\circ}$ and $45^{\circ}$,respectively. The influence of free stream velocity on the vibration, considering the turbulence intensity as a main parameter P. Hemon., et al, (2001), investigated the elongated cylinders in the galloping oscillation, with the shape ratio of 1:2. With the help of qualitative and quantitative flow visualization techniques, M. Ozgoren, et al, (2011), investigated the flow structures of a circular cylinder and sphere in a free stream flow. In other instant D. Jeon and M. Gharib (2001) conducted a set of experiments using both Digital Particle Image Velocimetry (DPIV) and force measurements techniques. Further D. Zuo, N.P. Jones (2009), attached two 27 by 27 cm square aluminum plates at the two ends of the cylinders to encourage two dimensionality of the impinging flow, for controlling the effects of finite length and the ends of the cylinders on the flow. Okajima, et.al (1999) evaluated the aero elastic instability of a circular cylinder with surface roughness, by free-oscillation tests in a wind tunnel. K. Matsuda et al., (2003) investigated the Flow-induced in-line oscillation of a 2-D circular cylinder model in a wind tunnel by the free-oscillation method to understand the fundamental characteristics of the system. Takayuki Tsutsui., (2012), carried out the flow visualization by smoke-wire and surface oil pattern methods. G.R.S. Assi et al., (2010), conducted an experimental investigation on a pair of circular cylinders to identify the effectiveness of pivoting parallel plates as a wake induced vibration (WIV) suppressors. The relationship between the performance and the characteristics of FIV was examined (K. Yakut et al. 2004). By using wind tunnel facility, an enormous number of experiments were examined by various researchers to study the behavior of FIV in the bluff bodies.

## Experimental Approach

In recent years, numerous studies on the FIV in the bluff bodies, especially in the circular cylinders were carried out in different phenomenon such as, the vortex shedding of stationary bluff body to the vortex shedding of an elastic body. The vortices generated due to the flow over the bluff bodies, resulted in the induced vibration which depend on various factors such as the vortex shedding frequency, Reynolds numbers, correlation of the force components, the material damping, the structural stiffness of the cylinder and the added mass effect. In this chapter, the summarization of experimental work which was conducted by many researchers so far has been described. For the different gap ratios Sarvghad-Moghaddam., et al, (2011), analyzed and calculated the pressure field, the vorticity distribution along with the associated streamlines and the time histories of hydrodynamic forces. While R.A. Kumar et al. (2008) performed an experimental analysis for various size ratios of test cylinder with the interfering cylinder values of 0.5, 1.0, 1.5 and 2.0, respectively. For a rigid cylinder G.R. Franzini et al., (2009), experimentally investigated, by mounting the bluff bodies on a low damping elastic base which was inclined in relation to the vertical, by an angle $\theta$ of $20^{\circ}$ and $45^{\circ}$,respectively. The influence of free stream velocity on the vibration, considering the turbulence intensity as a main parameter P. Hemon., et al, (2001), investigated the elongated cylinders in the galloping oscillation, with the shape ratio of 1:2. With the help of qualitative and quantitative flow visualization techniques, M. Ozgoren, et al, (2011), investigated the flow structures of a circular cylinder and sphere in a free stream flow. In other instant D. Jeon and M. Gharib (2001) conducted a set of experiments using both Digital Particle Image Velocimetry (DPIV) and force measurements techniques. Further D. Zuo, N.P. Jones (2009),

attached two 27 by 27 cm square aluminum plates at the two ends of the cylinders to encourage two dimensionality of the impinging flow, for controlling the effects of finite length and the ends of the cylinders on the flow. Okajima, et.al (1999) evaluated the aero elastic instability of a circular cylinder with surface roughness, by free-oscillation tests in a wind tunnel. K. Matsuda et al., (2003) investigated the Flow-induced in-line oscillation of a 2-D circular cylinder model in a wind tunnel by the free-oscillation method to understand the fundamental characteristics of the system. Takayuki Tsutsui., (2012), carried out the flow visualization by smoke-wire and surface oil pattern methods. G.R.S. Assi et al., (2010), conducted an experimental investigation on a pair of circular cylinders to identify the effectiveness of pivoting parallel plates as a wake induced vibration (WIV) suppressors. The relationship between the performance and the characteristics of FIV was examined (K. Yakut et al. 2004). By using wind tunnel facility, an enormous number of experiments were examined by various researchers to study the behavior of FIV in the bluff bodies.

## Wind Tunnel Facility

The wind tunnel is an effective tool to study the effects of the fluid (air) past the solid structures. The wind tunnel is classified into low speed, high speed, supersonic, hyper sonic, sub- sonic and the transonic wind tunnels. Different types of wind tunnels were equipped by various researchers in their research work to study the flow characteristics of fluids and its interaction with the solid structures. B.A. Jubran et al., (1998), conducted an experimental study in an open type wind tunnel with a square cross section area of 30cm x 30cm and a length of 200cm. Okajima, A., et al, (1999), experimentally investigated the bluff body (a circular cylinder) by mounting it on a working section of an open type low speed wind tunnel with the cross section of 0.3m x 1.2m. P. Hemon et al., (2001) inspected the FIV of the bluff bodies in test square section of 0.6m width (D) and 2m of length (L). Kitagawa, T., et al, (2002), conducted the experiments on the bluff bodies in a wind tunnel having the T-section of 1.8 m high and 1.5 m wide. Y.L. Lau et al., (2004), carried out the experiments in a closed circuit wind tunnel having a test-section of 2.3 m long and a square (0.6 m x 0.6 m) cross-section. A. Mohany, S. Ziada, (2005), examined in an open-loop wind tunnel having the test section made of 25.4 mm thick clear acrylic walls to facilitate a flow-visualization study in the future, with a cross-section of 76.2 mm in width x 254 mm in height. D. Sumner et al., (2005), conducted the experiments in a low speed, closed return type wind tunnel, with a test section of 0.91m (h) x 1.13m (width) x 1.96m (length). Ajith Kumar, R., Gowda, B.H.L,(2006.), examined the flow characteristics by placing the cylinder vertically at the center of the rectangular frame, supported by four springs in an open circuit wind tunnel with a square exit duct measuring 120mm x 120mm and the cylinders at a distance of 44 mm from the exit of the tunnel. Okajima, A., et al. performed an experiment analysis in a low speed and open type wind tunnel with a working section of 300mm x 1200mm. Further S. Pasto, (2008), performed the VIVs tests on a circular cylinder using a wind tunnel of a cross section 2.2 m wide and 1.6 m high. This was slightly divergent from the inlet to the test-section having the dimensions of 24m x 1.6 m with the global length of 24m from the inlet to the end of the diffusers of the wind tunnel. Md. Mahbub Alam, Y. Zhou, (2008), conducted the experiments in a low-speed, open-circuit wind tunnel with a test-section of 2.0 m x 0.35 m x 0.35 m. D. Zuo, N.P. Jones, (2009), conducted the tests in an open-return-type low turbulence (0.1% turbulence intensity) wind tunnel.

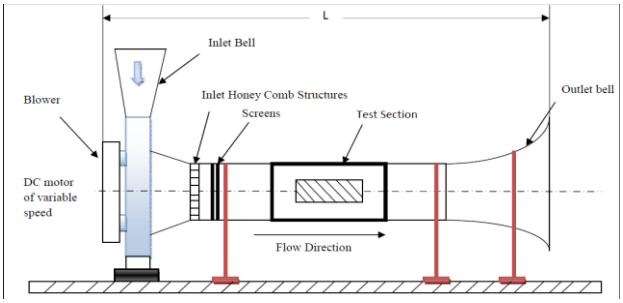


Fig.1. Experimental set-up: Sketch of wind tunnel.
(K.Karthik Selva Kumar & L.A.Kumaraswamidhas (2015))

S.C. Luo, R.X.Y. Tan, (2009), also performed the experiment in a smaller wind tunnel having a cross-section of 0.6 m (H) and 1 m (W) with the cylinder installed horizontally at the mid-height of the test section. S. Kim et al., (2009), carried out the free vibration test in a closed circuit rectangular wind tunnel with the test section of 0.35m x 1.2m x 3m (W x H x L), respectively and also carried out the flow visualization in a water channel with test section of 2m x 0.30m x 0.4 (L x W x D) to observe the flow structure around the vibrating Bluff bodies. P. Rojratsirikul et al., (2011), carried out the experiments in a low speed and closed loop open jet wind tunnel with a circular working section of 760 mm in diameter. In turn, S. Kim and S.C. Lee, (2012) carried out the free vibration tests in a closed-circuit rectangular wind tunnel with a test section having a width of 0.3 m, a height of 1.2 m and a length of 2.3 m to examine the characteristics of flow-induced vibration of a cylinder. Whereas, G. Schewe, (2013), carried out the experiments over a wide range of Reynolds numbers for a sharp-edged rectangular cylinder with the aspect ratio of height/width 1:5 (width/span ratio 1:10.8) in a high pressure (100 bars) wind tunnel.

### *A. Velocity and Turbulence intensity*

When a fluid past the bluff bodies, velocity and turbulence intensity has a significant impact in the development of FIV. The summarizations of research works at different velocity range with the turbulence intensity were reviewed. B.A. Jubran et al., (1998), performed the experiment with the free stream velocity which was varied from 4 to 27 m/s and with the free stream turbulence intensity level of 0.35%. Okajima, A., et al, (1999.), conducted the experiments in a wind velocity range of 1- 30 m/s with the turbulence intensity level of uniform flow in a work section less than about 0.5 %. P. Hemon et al., (2001), performed the experiments by varying the velocities from 4 to 30 m/s with the standard configuration of turbulence intensity between 0.4 % and 0.5 %, respectively. D. Wolfe, S. Ziada, (2003), conducted the experiments in a maximum flow velocity of 25 m/s and also performed at the flow velocity of 15.4 and 21.7 m/s, respectively. Y.L. Lau et al., (2004), carried out the experiments by setting the free stream velocity $U_\infty$ at 5.48

m/s. The turbulent intensity of the flow, entering the test-section, was about 0.025%. A. Mohany and S. Ziada, (2005) examined by equipping the blower with a 50 HP motor along with a variable speed controller to achieve a maximum flow velocity of 120 m/s in the test section. Whereas, Ajith Kumar, R and Gowda, B.H.L. (2006) conducted the experiments with the uniform fluid flow velocity over the 70% of the exit cross section with less than 1% variation. In turn, S. Pasto, (2008), investigated at the maximum velocity of U=35 m/s. Md. Mahbub Alam and Y. Zhou, (2008), experimentally simulated for a uniform flow in the test-section with the turbulent intensity of 0.5% at a free-stream velocity, U=14 m/s. S. Kim et al., (2009), researched on the FIV characteristics of two circular cylinders in tandem arrangement, with reduced velocity $U_r$ ranging from 1.5–26 m/s. In another instant, Prasanth T.K. and Sanjay Mittal, (2009), presented a comprehensive study by applying the reduced velocity ranging from 2 to 15 m/s. D. Zuo and N.P. Jones, (2009), conducted the experiments in an open-return-type low turbulence (0.1% turbulence intensity) wind tunnel test section of 0.91 by 1.22 m with a maximum wind speed of 71 m/s. G.R.S. Assi et al., (2010), conducted the experiment with the reduced velocity of the fluid flow up to nearly 30 m/s with turbulence intensity less than 3 %. M. Eid and S. Ziada, (2011), carried out the experiment at the reduced velocity range up to 10 m/s. P. Rojratsirikul et al., (2011), performed the experiments at the free stream velocity range of 5, 7.5 and 10 m/s. Takayuki Tsutsui., (2012), investigated the FIV on the bluff bodies at the free stream velocity, U, ranged from 6 to 20 m/s with the turbulent intensity of approximately 0.4% in this velocity range. G. Schewe (2013), investigated for the flow speed of U=38 m/s, along with an increasing range in turbulence intensity of the flow and also with a gradual increment in the flow speed and pressure. From the various studies it was observed that, to attain a standard smooth flow configuration, the turbulence intensity (I) must be around 0.3% to 0.5% for different velocity ranges, where the graphical representation of smooth flow configuration, suggested by P. Hemon et al., (2001) as shown in Fig. 2. The studies on FIV characteristics by L. Dubcova et al., (2008) at different velocity is discussed in the following section.For a far field of flow velocity ($U_\infty \leq 35$m/s), the displacement ($H$) and the rotation angle $\alpha$ are dying in time. When $U_\infty$ exceeds 30 m/s, then the damping of the flow-induced vibrations becomes weaker and at about $U_\infty \approx 40$ m/s the system becomes unstable by fluttering, the vibrations amplitudes become so high that it exceeds more than 100 mm and 15◦ at a limit cycle oscillation (see Fig. 3)

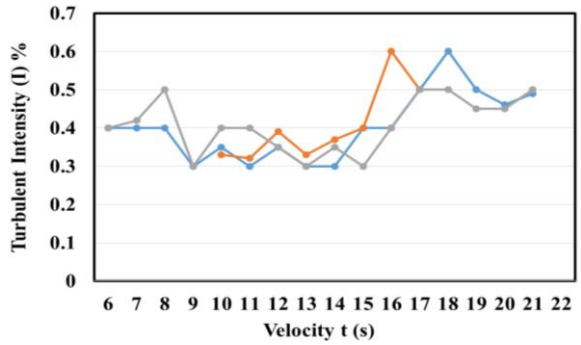


Fig.2. Turbulence intensity v/s wind velocity for the smooth flow configuration, (P. Hemon et al., 2001)

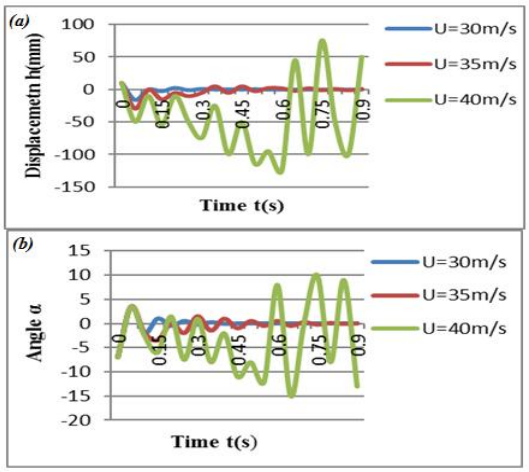


Fig.3. (a) & (b) shows the Flow-induced vibrations characteristics for the velocity, $U_\infty$ = 30m/s,35m/s, 40 m/s.(L. Dubcová et al., 2008)

*i. Bluff Bodies*

Bluff bodies are solid structures such as circular, square, rectangular etc. applicable for all engineering and non-engineering aspects. A comprehensive study by various researchers on the FIV in the bluff bodies for studying the performance of different structures under the forced fluid flow are summarized in this section. B.A. Jubran et al., (1998), tested the cylinder made of an aluminum tube with the cross section having an outer diameter D as 21.5 mm, wall thickness t as 0.5 mm and the length L of 440 mm. Kitagawa, T., et al, (2002), examined the two circular cylinders having identical cross section diameters of 50 mm each with the height of 1320mm. K. Matsuda et al., (2003), performed the analysis on FIV in two cylinders having equal diameters of 200mm with varying length of 356mm, 1354mm, respectively. Y.L. Lau et al., (2004), used a slender NACA0012 airfoil which was placed downstream of the cylinder. A. Mohany, S. Ziada, (2005), investigated that the bluff body which is made of aluminum was machined to produce a qualitatively similar surface roughness for all cylinders. Z.J. Wang, Y. Zhou, (2005), analyzed the bluff body made of two side-by-side acrylic circular tubes with an identical diameter of d = 10 mm. Whereas Ajith Kumar R. and Gowda B.H.L. (2006), used an aluminum tube with a square cross section of side 12 mm, wall thickness 1 mm and length 140 mm. A. Okajima et al, tested the models which had a diameter of D=160 mm with a span of 293 mm made of acrylic acid resin and also reviewed the FIV of two identical circular cylinders, having the diameter D of 120 mm with the span length of 293 mm which was made of Styrofoam where its smooth surfaces are covered with aluminum foil. S. Pasto, (2008), utilized a 23m long circular hollow cylinder having a diameter of about 0.155 m. A.P. K.M. Lam, (2007), performed the experiments on two rigid aluminum cylinders having the effective lengths of 32 cm with the cylinder diameters of (D) 3.2 cm and (d) 1.6 cm. Md. Mahbub Alam, Y. Zhou, (2008), performed the experiments on two brass cylinders with the diameters (D) 25 mm and (d) of 25, 20, 15, 10 and 6 mm, respectively, which were mounted in tandem

arrangement, vertical to the mid-plane of the working section. S. Kim et al., (2009), investigated two circular cylinders having identical diameters of 66 mm each, made up of polyurethane and it was also covered with an aluminum plate of 0.2 mm thickness. S.C. Luo, and R.X.Y. Tan, (2009), inspected a circular cylinder made up of brass, which had a highly polished surface having the diameter (d) of 25 mm with a length in excess of 1 m. D. Zuo, N.P. Jones, (2009), the sectional models tested, were hollow circular PVC tubes 0.091 m in diameter and 2.14 kg/m in mass density. Prasanth, T.K., Sanjay Mittal, (2009), examined the FIV on the bluff body having the diameter of 100 mm. G.R.S. Assi et al., (2010), analyzed the Perspex tube of circular cylinder models having the diameter of 50 mm. P. Rojratsirikul et al., (2011), tested a rectangular wing model with an aspect ratio of AR=2, and a chord length of c=68.8 mm. The bluff body used in the free vibration test was 66 mm in diameter (d) and had an aluminum shaft of 10mm in diameter at the center of the cylinder which was made up of paper to reduce the weight and wrapped by a 0.2 mm thick aluminum plate (S. Kim and S.-C. Lee, 2012). Takayuki Tsutsui., (2012), investigated the FIV behavior in a circular cylinder having a diameter of 100mm with the span length of 150 mm, respectively.

*ii. Techniques used to observe different parameters during the Experimental Analysis*

Different techniques adopted by various researchers to observe and analyze the frequencies of FIV on the bluff bodies are summarized in this section. B.A. Jubran et al., (1998), performed with a piezoelectric accelerometer (type: B&K 4370) placed on one end of the test cylinder where the output signal from this accelerometer was simultaneously fed to a portable (B&K 2626) type conditional amplifier. The output of the conditional amplifier was fed to a computer via an interface card (type: I Lab PC+). To measure the flow induced structural vibration. Jin et al, (2000), suggested the fiber grating sensor as an alternative technique. In another work P. Hemon et al., (2001), examined the turbulence and wake, by mounting a single channel hot anemometer by which a calibration curve of 4 order polynomial was observed, subsequently, the data was acquired on a Pc using high speed A/D converter with the sampling frequency up to 400 kHz. In other sequence of research works, P. Hemon et al., (2001) measured the free vibrations by using piezo-electric sensors glued on middle upper face on the beam of 40 mm thick, which was further connected to the data acquisition system through a charged amplifier with an analog filter. In turn, the charged amplifier was wired to deliver a dynamic signal, representing the velocity of the structure at the location of the sensor, thus the signal voltage is zero when the beam is not moving. This type of measuring method was mostly chosen to eliminate zero shift problems by thermal or pre-stress effects. Where K. Lam et al., (2003), applied a piezo-electric load cell to measure the force coefficient and Strouhal numbers (St) on four cylinders in a square configuration at a subcritical Reynolds number range, simultaneously analyzed the flow around the four cylinders in a square configuration using laser-induced fluorescence (LIF) visualization and the Particle Image Velocimetry (PIV) for angles of incidence ranging from $\alpha = 0° - 45°$ at a rate of $5°$ interval and also adopted the LDA technique to capture the velocity distributions during the fluid flow past the bluff bodies. With the help of laser vibrometer Y.L. Lau et al., (2004), measured the bending and torsional vibration displacement in the mid-span of the airfoil and cylinders. For further studies, Ajith Kumar, R., Gowda, B.H.L.(2006), performed the analysis with one of the springs supporting the cylinder, in turn, it was connected to a dynamic pick up (Type 8001; Bruel and Kjaer) further connected to a storage oscilloscope (Type 1744A; Hewlett Packard) through a charged amplifier (Type 2626; Bruel and Kjaer). S. Kim et al., (2009), measured the vibration displacement of the cylinder by a laser displacement meter and Flow velocity, by using a propeller-type velocity meter. A. Mohany and S. Ziada calibrated the flow velocity inside the test-section with a Pitot tube and a pressure transducer where the results were observed by placing the microphone at the maximum acoustic pressure location and also evaluated the spectral analysis with the help of Hewlett Packard analyzer. I.C. Chu et al., (2011), carried out the study with the ten 3-axis accelerometers for the measurement of vibration responses.

K.Karthik Selva Kumar & L.A.Kumaraswamidhas (2015)) experimentally investigated in an open type low turbulence (0.1% turbulence intensity) wind tunnel at the Fluid Flow Laboratory of Indian School of Mines University (ISMU). The wind tunnel has test section of 0.3m x 0.3m x 1.0m, with a maximum wind speed up to 75 m/s. The temperature of the fluid flow was at 22°C. In turn, prior to the 9:1 contraction a layer of honeycomb and some screens were installed to reduce the turbulence. At the opening of the test section, a pitot tube was equipped to monitor the inlet fluid flow velocity. The Reynolds number based on the inlet flow velocity and the diameter of the test cylinder is $1.6 \times 10^4$. The flow velocity distribution without considering the boundary layer in the test section area is found to be even within 1.1%. The section models tested were hollow circular copper tubes of diameter D=12mm and span length of 150mm were used as a test cylinders and the ratio of the cylinders centre to centre gaping with respect to the diameter of the cylinder (P/D) is 1.55. Apart from the elastically mounted circular cylinder at the centre, the adjacent cylinders were mounted rigidly in a 60° rhombus triangular pattern. To visualize the fluid flow around the test cylinder surface, a smoke generator with a small orifice was placed at a half a diameter of the cylinder distance in the upstream condition. The orifice of the smoke generator was located at the mid-span of the cylinders and about the similar height of the cylinder axis in mid-span. As shown in the Fig 5, for each case other than the surrounding tube bundles, the test cylinder mounted at centre is equipped with two accelerometers in the top edge and bottom edge. Whereas in the present study, the natural frequency of the surrounding cylinders were fixed at $f_s = 24$ Hz and the natural frequency of the test cylinder $f_n$ was set at 12 Hz ($=1/2\,f_s$), 18 Hz ($=3/4\,f_s$), 24 Hz, and 30 Hz ($=5/4\,f_s$) for tests with different natural frequencies. The instrumentation set up includes two accelerometers manufactured by B&K having sensitivity of 100 mV/sec$^{-2}$ with the frequency response up to 0.3-8 kHz. The two accelerometers were installed at the each edge of test cylinder elastically mounted in the centre. The orientation of the accelerometers were adjusted according to their sensitive with respect to the tube vibration

in the stream wise (X) and cross Flow (Y) direction respectively. Further the observed output from each accelerometer was analyzed by employing a B&K 2 channels dynamic signal analyzer as shown in the figure 3.

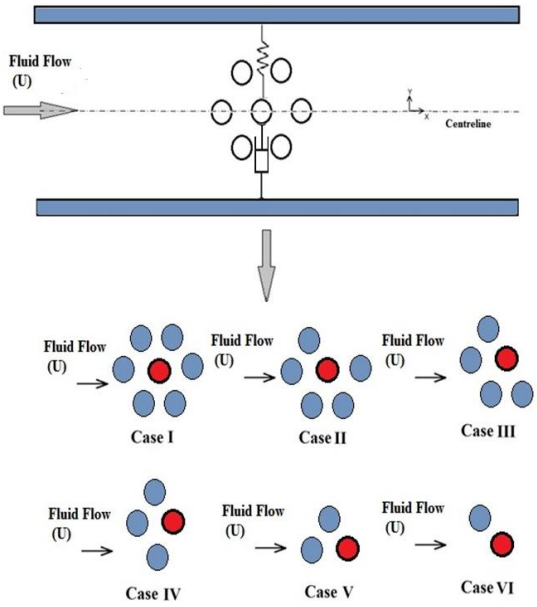


Fig.4. Test cylinders at different configurations. (K.Karthik Selva Kumar & L.A.Kumaraswamidhas (2015))

The obtained X and Y displacement signals were digitized simultaneously at a sampling rate of 192K samples/sec by a 24 bit ADC, whereas the B&K signal analyzer is connected to a PC computer to store the data for further processing and to monitor the amplitude spectra of the test cylinder during the experimental investigation. Before measuring the vibration excitation in the test cylinder, the voltage outputs from the data acquisition and signal analyzer system is calibrated in opposition to the vibration amplitudes. While calibration, the test cylindrical copper tube with the two accelerometers at each edge was given a circular motion. Besides that, a distinctive time series of displacements in the stream wise (X) and cross flow (Y) direction are shown in Fig. 6(a). The amplitudes with respect to the sinusoidal output voltages for the stream wise (X) and Cross flow (Y) directions were observed and then plotted in opposition to the vibration amplitude. As shown in Fig. 6(b), the calibration data for both the stream wise (X) and cross flow (Y) directions are fixed to a straight line V = aA + b, where A represent the vibration amplitude and V represents the voltage output. Curve-fitting gives the values of the coefficients, a = 0.11 and b = 0.008. It is thus shown that the voltage outputs can linearly represent the vibration amplitudes in the experimental range. To distinguish the enormity of the test cylinder vibration, the real mean square value with respect to the vibration amplitude ( $A_{rms}$ ) is expressed in a dimensionless form as,

$$(A_{rms} / D) = \sqrt{x_{rms}^2 + y_{rms}^2} / D \qquad (1)$$

Where the diameter of the cylinder is represented as D, rms values of the cylinder displacement in x and y direction is represented as $x_{rms}$ and $y_{rms}$ respectively.

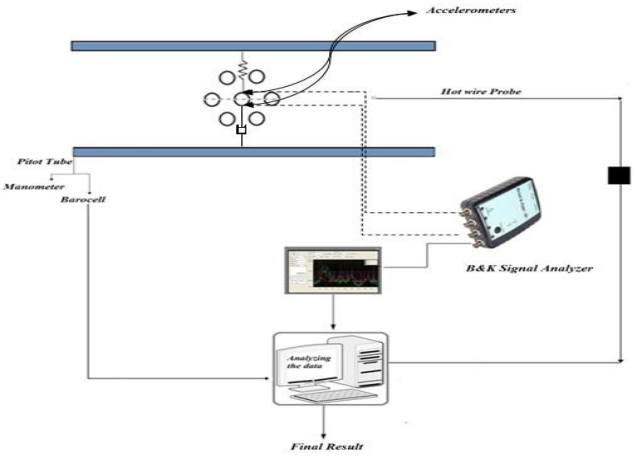


Fig.5. A sketch of data acquisition and signal measurement setup. (K.Karthik Selva Kumar & L.A.Kumaraswamidhas (2015))

The cylinder displacements were observed by digitizing the yield voltages observed from the measurement system which transforms the cylinder displacement into voltage signal. Whereas, the fine accuracy of the vibration measurement and data acquisition system resulting in causing uncertainties in the measurement of displacement of the cylinders in x and y direction.

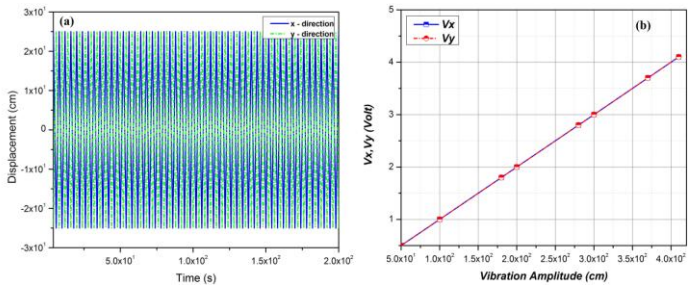


Fig.6. (a) Displacement in x and y direction, (b) output voltage *Vx* and *Vy* versus vibration amplitude in x and y direction (K.Karthik Selva Kumar & L.A.Kumaraswamidhas (2015))

*B. Arrangement of Bluff Bodies*

The arrangement of the bluff bodies in the direction of fluid flow has a significant effect in the study of FIV characteristics. Three types of arrangements have been studied so far, the tandem arrangement, staggered arrangement and the side-by-side arrangements. In cases of more complex arrangements, investigations of the flow around pairs of cylinders can provide much better understanding of the vortex dynamics, pressure distribution and fluid forces. (Ajith Kumar, R., Gowda, B.H.L.), performed the investigations of the flow around the interfering cylinders arranged in tandem and staggered arrangements were made out of solid aluminum rods with a smooth finish and square cross-section with a length of 140 mm and side dimension ratios (b/B) of 0.5, 1.0, 1.5, respectively. (Meneghini, J.R., et al 2001), investigated the vortices shedding and the flow interference between two

circular cylinders in tandem and side-by-side arrangements. The flow configuration for the cylinders in tandem, staggered and side-by-side arrangements are shown in the Fig 7.

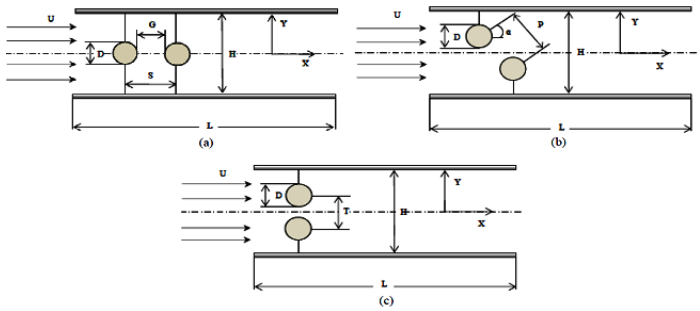


Fig.7.The Flow configuration for the circular cylinders of equal diameter in (a) tandem arrangement. (b) Staggered arrangement. (C) Side by Side arrangement.

*i. Tandem Arrangement*

The tandem configuration is nothing but the bluff body's sequential arrangement, where the research works done by different researchers so far, have been done on the FIV in the bluff bodies, arranged in tandem configuration, has been discussed in this chapter. In order to investigate the wake interference effect on the strake efficiency, an experimental arrangement with two or multiple cylinders in tandem, must be employed. Gheorghe Juncu (2007) performed a computational study of the steady, axisymmetric, viscous flow around two circular cylinders in tandem. T. Kitagawa., H. Ohta., (2008), performed a three dimensional fluid computation to investigate the flow around the circular cylinders in tandem arrangement. In turn, by varying the Centre-to-Centre distance (S/D) of the cylinders from 2 to 6, Korkischko, I. and Meneghini, J.R. studied the fluid dynamics in the tandem arrangement. B.S. Carmo, et al, (2011), performed a 2 and 3-dimensional numerical simulations of the flow around two circular cylinders in tandem arrangements. Lam, K., et al (2012) did a comprehensive study on the turbulent flows around two fixed unyawed and yawed wavy cylinders in the tandem arrangement. With respective to the incident uniform flow, B.S. Carmo et al., (2013) studied the flow characteristics around the two circular cylinders of equal diameter, arranged in a tandem configuration. The instantaneous pressure field around the two circular cylinders arranged in the tandem arrangement was investigated by J. Lin, et.al. (2013) and also performed the flow visualization in order to clarify the behavior of the gap flow and the oscillating fluid force. From the review it was identified that in some cases the displacement of the front cylinder is larger than that of the rear one, while in most cases the rear cylinder suffers larger amplitude oscillations. S.Bhattacharyya and S. Dhinakaran studied the flow of incompressible fluid past a pair of square cylinders in tandem, placed close to a flat wall. Similar to that of a single cylinder at all reduced velocity U* Prasanth, T.K., Sanjay Mittal found out that the cylinders in tandem arrangement undergo a figure such as numeric '8' motion.

*ii. Staggered Arrangement.*

The summarization of the research work on FIV in the bluff bodies arranged in staggered configuration by various researchers is discussed. D. Sumner et al., (2005), measured the mean aerodynamic forces and vortex shedding frequencies for two circular cylinders of equal diameters in staggered arrangement. The effect of free vibration and the flow-visualization of the two cylinders in staggered arrangement were studied, in both stationary and oscillated cases, (Ajith Kumar, R., Gowda, B.H.L.,). Where Prasanth, T.K., Sanjay Mittal performed the experimental investigations in staggered arrangement for the centre, to centre distance S/D as 0.7. In this arrangement the downstream cylinder is expected to lie in the unsteady wake of the upstream one. From the studies it was found that in staggered arrangement, the upstream cylinder undergo a figure of numeric '8' and the motion was similar to that of a single cylinder at all free stream velocity U*. In turn the downstream cylinder was found to undergo two types of motion: (i) an orbital motion and (ii) figure of numeric '8' motions.

*iii. Side-by-Side Arrangement*

This chapter deals with the summarization of the research work on the bluff bodies in side-by-side configuration by various researchers. Wang, Z.J and Zhou, Y experimentally investigated the flow behind two side-by-side circular cylinders. In another instant Meneghini J.R., et al (2001) carried out the simulations of two cylinders in side-by-side arrangement for the gap ratio in the range of 1.5D<L<4D. Where S. Ryu et al., (2009), estimated the hydrodynamic coefficients for the fluid flow around cylinders in side-by-side arrangement with respect to the variation in separation gap. In turn, F.J. Huera-Huarte and M. Gharib (2011) studied the FIV on two vertical cylinders in side-by-side arrangement.

*C. Flow Motion/Direction*

The separation of the bluff bodies in the stream flow had a significant influence on the motions of flowing fluids; with the variation in the gap ratio it was observed that there were different flow patterns in the fluid flow, past the bluff bodies. The variety of distinct vibration regimes involving periodic, quasi-periodic and non-periodic vibrations with corresponding flow patterns and the responses of the cylinders are classified into three distinct categories as: (a) The instability builds up rapidly to the large-amplitude oscillations primarily in the stream wise direction, (b) The instability builds up slowly to a certain amplitude with oscillations mainly in the stream wise direction and (c) The instability grows gradually to large oscillation amplitudes primarily in the cross-flow direction. Whereas Wang, Z.J and Zhou, Y classified the flow into three regimes according to the T/d ratio as: single street (the cylinder center-to center spacing T/d < 1.2), asymmetrical flow (1.2 < T/d < 2.0) and two coupled streets (T/d > 2.0).It was also observed that the gap bleeding between the cylinders play a significant role in determining the flow pattern behind the cylinders. Prasanth, T.K and Sanjay Mittal, compared the response of the cylinders in tandem and staggered arrangements to each other and with that of an isolated cylinder. Kitagawa, T., et al, measured the transverse dynamic response of a rocking circular cylinder and showed the occurrence of that vibration around a wind speed about three times higher than the threshold wind speed of VIV and is known as the end-cell-induced vibration (ECIV). When the fluid-elastic effects are

not significant and are restricted to the added mass effects, then there is no strong coupling between structure and fluid motion, wherein the structure displacement is not supposed to affect flow patterns, (Longatte, E., et al). Y. Bao et al., (2011), examined the flow interference by scrutinizing (i) the frequency characteristics of the vortex shedding and oscillation; (ii) the dynamic response of the oscillating cylinder, including the amplitude of displacement, the drag and lift force characteristics and the phase relationship between the lift and the displacement series; and (iii) the flow response in terms of the instantaneous vorticity field. The results show that the type of flow interference is significantly affected by the angle of the incident flow. The flow motions are classified into transverse or cross flow and stream wise direction.

*i. Transverse (Cross - Flow) direction*

The flow over two tandem cylinders which is moving freely in transverse direction in parallel-wall channels will result in a novel type of induced vibrations. The summarization of work done in cross-flow is discussed in this section; obviously the investigation on the cylinders or the bluff bodies is undertaken by separating it at 0.7D in the cross-flow direction arranged in staggered configuration Prasanth, T.K., and Sanjay Mittal found out that the transverse response of downstream cylinder was highly different from the upstream one. Whereas Okajima, A., et al. measured the response amplitudes but for the roughened cylinder oscillating in the transverse (cross flow) direction of the fluid flow. D. Wolfe, S. Ziada, (2003) investigated the feedback control on vortex shedding from two cylinders arranged in tandem configuration in the cross-flow direction. A. Joly et al., (2012), validated the model efficiency and its predictions to the unsteady simulations of the fluid–structure interaction of a spring mounted square, constrained to move in the direction transverse to the flow. Assi, G.R.S., et al, (2006), performed the experimental investigation in cross flow direction. G.R.S. Assi et al., (2010), measured the amplitude of vibration and presented the average drag for a circular cylinder which was free to respond in the cross-flow direction. K. Schroder, H. Gelbe, (1999), studied 2-D and 3-D simulation models for the computation of flow-induced vibration in the tube bundles which were subjected to the single-phase cross-flow.

*ii. Stream wise direction*

The summarizations of the significant work performed in the stream wise direction in the recent years were as follows. J. Lin et al. (2013) investigated the bluff bodies in stream wise direction in a plane channel using the lattice Boltzmann method. Prasanth, T.K., Sanjay Mittal, performed the investigation by separating the cylinders in stream wise direction. The non-dimensional distance between the centers of the two cylinders is denoted by P/D.

*D. Dimensionless Parameters*

*i. Reynolds Number*

The Reynolds number (Re) is a dimensionless parameter which measures the ratio between the inertial forces to the viscous forces. S. Pasto, (2008), classified the Reynolds number (Re) into Subcritical range ($300<Re\leq 1.5x10^5$), Critical range ($3x10^5<Re\leq 3.5x10^6$) and Super critical range ($Re>3.5x10^6$) as important regimes among all the other regimes of the Reynolds numbers and also stated that the vortex shedding is mostly affected due to the Reynolds number. Whereas Okajima, A., et al, simulated the flows at low wind velocity at high Reynolds numbers by introducing the surface roughness. J. Lin et al. (2013) performed the experiments at fixed Reynolds number (Re) of 100. The classification of Reynolds number is shown in Table 2, as follows:

TABLE.2. Classification of Regime according to Reynolds number range.

| S. No | Regime | Reynolds Number Range |
|---|---|---|
| 1 | The Periodic laminar wake | $30<Re<150$ |
| 2 | The Subcritical regime | $150<Re<1.4 \times 10^5$ |
| 3 | The Critical regime | $1.4 \times 10^5< Re < 1 \times 10^6$ |
| 4 | The Supercritical regime | $1x10^6<Re<5x10^6$ |
| 5 | The Trancritical regime | $5x10^6<Re$ |

The Reynolds numbers were based on free stream velocity of the fluid and the diameter of the cylinders, (Prasanth, T.K., Sanjay Mittal), (M. Ozgoren et al, 2011) & (Sarvghad-Moghaddam., et al, 2011). (K. Lam et al, 2003), (J. Lin et al. 2013) & (Meneghini, J.R., et al 2001), performed the experimental analysis at the Reynolds number range of 100 to 200, respectively, L. Baranyi, performed the numerical simulation for the flow past a circular cylinder in orbital motion at the low Reynolds number flow (Re = 120–180).

*a) Subcritical Reynolds Number*

The research work performed at the Subcritical Reynolds number ranging of $150<Re<1.4 \times 10^5$is summarized in this chapter. Fenghao WANG, et al., (2008), simulated the flow-induced vibrations for the four tubes in a rotated square, arranged in a staggered tube bundle in three rows and five columns, at the high sub-critical Reynolds number (Re) range. Where (Z.J. Wang, Y. Zhou), (S. Mittal and V. Kumar, 2001), (C. Norberg, 2003), (Y.L. Lau et al., 2004), (S. Dong, G.E. Karniadakis, 2005), (Assi, G.R.S., et al, 2006), (S. Atluri, et al., 2009), (S.C. Luo., R.X.Y. Tan,, 2009), (Korkischko, I., Meneghini, J.R, 2010), (WANG Jia-song, 2010) & (Lam, K., et al, 2012), performed the experimental investigations of the FIV on the bluff bodies at the Reynolds number range of 1000 to 16,000. (G.R.S. Assi et al., 2010), (Kitagawa, T., et al), (Md. Mahbub Alam, Y. Zhou, 2008), (T. Kitagawa., H. Ohta., 2008), and (P. Rojratsirikul et al., 2011), performed their experimental investigation of FIV on the bluff bodies at the Reynolds numbers range (Re) of $2.4 \times 10^4$–$4.8 \times 10^4$ , respectively. (Fenghao WANG, et al., 2008), performed the study with a fluid-structure Interaction model based on SVM for the FIV on tube bundles in a medium space ratio at $Re = 2.67 \times 10^4$. (Okajima, A., et al), (D. Sumner et al. 2005), (D. Wolfe, S. Ziada, 2003), (B.A. Jubran et al., 1998), (B.A. Fleck, 2001), (M. Eid, S. Ziada, 2011), (S. Kim et al., 2009), were investigated at the Reynolds number range of $4 \times 10^3$ to $1 \times 10^5$.

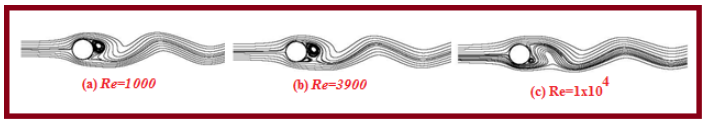


Fig.8. Instantaneous Streamlines at different Reynolds numbers

*b) Critical Reynolds Number*

The research work performed at the Critical Reynolds number ranging from 1.4 x $10^5$< Re < 1 x $10^6$is summarized in this chapter. A. Joly et al., (2012), performed the experimental analysis and the software simulation of FIV of the bluff bodies. Takayuki Tsutsui, (2012), performed the experimental investigation at the Reynolds number ranged from 3.8 x $10^4$ – 1.3 x $10^5$, where the Strouhal number decreases from 0.25 to 0.10, as the Reynolds number increases.

*c) Super Critical Reynolds Number*

The research work carried out at the Super Critical Reynolds number ranging from $1x10^6$<Re<$5x10^6$ is summarized in this chapter. M.C. Ong et al., (2009), performed the experimental analysis at high Reynolds number flow (Re = 1 x $10^6$, 2 x $10^6$and 3.6 x $10^6$, based on the free stream velocity and the cylinder diameter) covering the supercritical Reynolds number to upper-transition flow regimes around a 2-D smooth circular cylinder. Raghavan, K., and Bernitsas, M.M., conducted the experiments in the regime right before transition from the laminar to the turbulent flow at high-Reynolds numbers range ($2xl0^4$- 4 x $l0^4$ < Re < 3.5 x $l0^5$- 6 x $l0^6$).

*ii. Mass Ratio*

The mass ratio is the measure of efficiency of the bluff bodies. J. Lin et al. (2013), performed the experiment analysis with the mass ratio of m* = 0.1 and 1, respectively. (Prasanth, T.K., Sanjay Mittal), studied the fluids, characteristics with a mass ratio m* of 10. Korkischko, I., and Meneghini, J.R, performed the experimental analysis with a mass ratio of m* = 1.8 for all models. (Y. Bao et al., 2012) and (G.R.S. Assi et al., 2010), carried out the computation with a low reduced mass ratio of m*=2. K. Ryan et al., (2004), performed 2-dimensional simulations of the flow past a tethered cylinder with a mass ratio m* = 0.833. The vibration frequency becomes innately large because the mass ratio reduces to a limiting value of 0.54 T. C.H.K. Williamson, and R. Govardhan (2008) concluded that the Critical mass ratio $m^*_{CRIT}$ = 0:54 ± 0:02, and below that, the lower branch of response can never be reached for finite velocities. These conditions are applicable for the finite U*/f*.

*iii. Blockage Ratio*

The blockage effects were mainly due to the ratio of the dimension of the bluff bodies to the dimensions of the wind tunnel cross section, (D. Zuo and N.P. Jones, 2009).The blockage has a very significant impact on the response of the bluff bodies undergoing vortex-induced vibrations, a blockage greater than 2:5% can lead to the hysteresis in the flow and response of the bluff bodies at the onset of synchronization, where higher blockage ratio also leads to an error in the whole process. The summarizations of blockage ratio obtained by various researchers are shown in the fig. 9. For normal flow process the blockage must be lesser than 2.5%.From the fig. it was observed that the blockage ratio obtained by various researchers more than 2.5 % have faced the hysteresis in the flow which might lead to an error in their work progress.

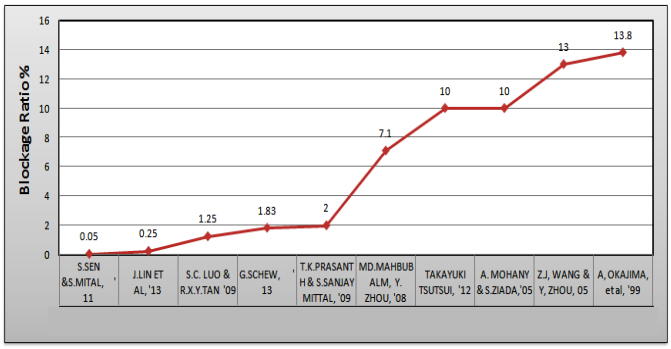


Fig.9. Blockage Ratio observed by various researchers.

*iv. Structural Damping*

The damping is an effect of reducing the amplitude of oscillations in an oscillatory system or structure. The setting of structural damping parameters was having a significant effect in reducing the amplitude of oscillation in the structure due to fluid flow. To encourage the high amplitude of oscillation in turn maximizes the vortex induced response of the bluff bodies (Prasanth, T.K., Sanjay Mittal), (J. Lin et al. 2013) and (Y. Bao et al., 2012) fixed the structural damping parameter as zero. In turn K. Matsuda et al., (2003) performed an experimental analysis with the structural damping ratio of (0.5 to 0.18) and (0.005 to 0.023), respectively.

*v. Spacing Ratios*

The spacing between the structures during the fluid flow plays a vital role in resulting induced vibration. The research work performed in various spacing ratios is summarized in this chapter. Fenghao WANG, et al., (2008), used a fluid-structure interaction model based on the Surface Vorticity Method (SVM) to study FIV of the tube bundles in a minimum space ratio. V. Kumar and S. Mittal, (2001) carried out the experimental analysis on the fluid flow around the bluff bodies, in stream wise direction the cylinders arranged in a staggered manner, was separated by 5.5 times the cylinder diameter and for cross flow the spacing between the two cylinders was 0.7 times the cylinder diameter. Prasanth, T.K., and Sanjay Mittal carried out the investigation in both staggered and tandem arrangement and the cylinders were separated by 5.5D in the stream wise direction. S. Bhattacharyya and S. Dhinakaran noted that the critical value of Reynolds number (Re) was depending upon the spacing ratio of the cylinders. Md. Mahbub Alam, and Y. Zhou, (2008), carried out the investigation of flow past the bluff bodies at the spacing ration of 5.5D. Z.J. Wang, and Y. Zhou, carried out the experiments at three transverse spacing ratios of T/d = 3.00, 1.70 and 1.13. (K. Lam et al., 2003) and (D. Wolfe, S. Ziada, 2003), conducted the experiments at the spacing ratio of 4D and 4:5D, respectively. A. Vakil, S.I. Green, (2011), investigated the flow around the side-by-side

arranged cylinders with the surface-to-surface separation ratio in the range 0.1 < s/D < 30 of the cylinder diameter. Y. Bao et al., (2013), carried out the simulation for four cylinders with the spacing ratio ranged from 1.2D to 4.0D, corresponding to the four kinds of wake pattern for the two stationary cylinders, where the variation of spectral contents of St numbers for the cylinders with gap spacing, were shown in the fig. 10. From the above graphical representation, it was identified that the upstream cylinder having the Centre to Centre spacing ratio S/D=1.2, is exhibiting a high level fluctuation than the others. In another instant Sarvghad-Moghaddam., et al, (2011), carried out the computational simulations for the different transverse gap ratios ($1.5 \leq T/D \leq 4$) in laminar (Re=100 and 200) and turbulent ($Re=10^4$) regimes, in which the $T$ and $D$ represents the distance between the centers of cylinders and their diameters, respectively. D. Sumner, (2010), noted that the longitudinal and transverse spacing between the cylinders had a strong influence on the parameters such as flow patterns, aerodynamic forces and the vortex shedding. (F.J. Huera-Huarte, M. Gharib, 2011) and (Y. Bao et al., 2012), carried out the investigation on the cylinders at side-by-side arrangement and tandem arrangement, respectively, with a spacing ratio of 5D. Lam, K., et al, (2012), investigated at a range of the cylinder spacing (L) between the cylinders from $1.5D_m \leq L \leq 5.5\ D_m$ with yaw angles of $\alpha = 0^0, 30^0$ to identify the effects of the cylinder spacing ratio and the yaw angle as well as the coupling effects of the two wavy cylinders in the tandem arrangements.

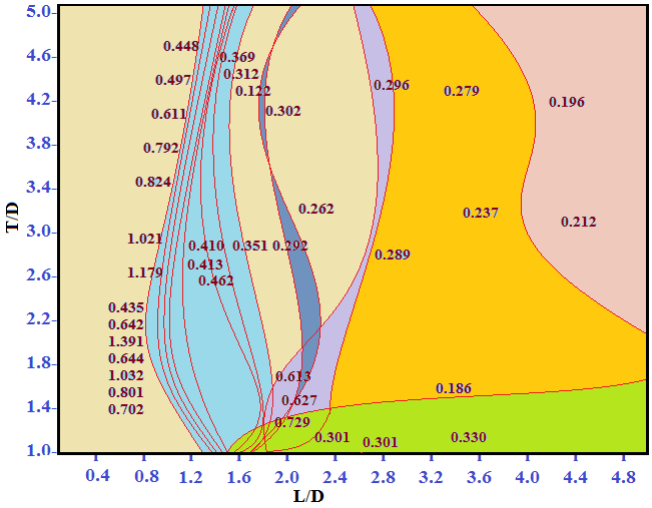


Fig.**10**. Fluctuation in the St at different spacing conditions, T/D & L/D. (K.Karthik Selva Kumar & L.A.Kumaraswamidhas)

With the help of the laser-induced fluorescence visualization technique K. Lam et al., (2003), investigated at the six spacing ratios (L/D) varying from 1.69 to 3.83 with 13 different angles of incidence, ranging from $0° - 180°$ at an $15°$ interval, covering all the orientations. Carmo, B.S., et al., (2013), performed the 2-D and 3-D simulation for the bluff bodies in tandem arrangement at the spacing ratio of L/D =4. J. Deng et al., (2007), noted that the critical spacing ratio was found to be L/D=3. A. Mohany and S. Ziada, investigated the effect of gap between the cylinders at eleven spacing ratios in the range of L/D = 1.2 – 4.5, respectively. S. Kim et al., (2009), investigated the FIV characteristics of two circular cylinders in tandem arrangement at five spacing ratios of L/D = 0.1, 0.3, 0.8, 2.0 and 3.2.

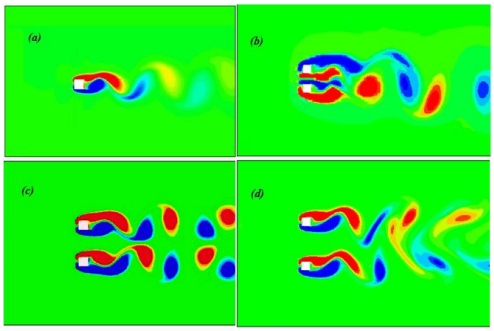


Fig.11. (a) Flow characteristics of single square cylinder, (b) Flow characteristics of elastically mounted side by side square cylinders at T/D=1.0, (c) Flow characteristics of elastically mounted side by side square cylinders at T/D=3.5, (d) Flow characteristics of elastically mounted side by side square cylinders at T/D=4.5. (K.Karthik Selva Kumar & L.A.Kumaraswamidhas (2014))

Iman Harimi, and Mohsen Saghafian, performed at different spacing ratios of L/D at 2, 3, 4, 5, 7 and 10, respectively. K. Matsuda et al., (2003), carried out the investigation for the two circular cylinders at the aspect ratio of L/D of 1.8, 6.8, respectively. (A. Joly et al., 2012) and (Takayuki Tsutsui., 2012), performed the investigation on the flow past cylinders at the spacing ratio of L/D (1.2 to 1.3) and at approximately equal to 3, respectively.

*vi. Mass Damping Parameter (Scruton Number)*

The mass-damping parameter was first introduced by Scruton in 1955 for the purpose of the characterization of the flow-induced vibration of the cantilevered flexible structures with the interference of wind, afterwards it was quickly adopted by various researchers then Scruton number was expressed as Sc,

$$S_C = \frac{2m\delta}{\rho D^2} = \pi^2 m^* \zeta \qquad (2)$$

In turn, Griffin and colleagues, made an attempt to expand the application of the mass-damping parameter for the prediction of the maximum response amplitude in a wide variety of the flexible structures, including the cables equipped in hydel application. Finally, the new parameter Skop-Griffin parameter was derived as SG

$$S_G = 2\pi S^2 k_S = 2\pi S^2 \frac{2m\delta}{\rho D^2} = 2\pi^3 S^2 m^* \zeta \qquad (3)$$

The amplitude response was measured by K. Matsuda et al., (2003) over a wide range of the mass-damping parameter which was found to be (0.8 to2.9) and (0.9 to 4.2), respectively. Where G.R.S. Assi et al., (2010) measured the response amplitude of damping parameter at the range of 0.7% of critical damping. (Ajith Kumar, R and Gowda, B.H.L) and (Okajima, A et al), performed the experimental analysis for the mass damping parameter $k_s$ (Scruton number) of 3.2 and 6, respectively. The dimensionless damping parameter for the cylinders experiencing the flow-induced vibration was defined as,

$$C^* = 2\omega / \rho U^2 \quad (4)$$

In which the damping parameters are not well-suited for the response of flexible cylinders in sheared flows or the cylinders were equipped with strakes or fairings.

## Analytical and Numerical Approach

Analytical and Numerical studies on the FIV in the bluff bodies by researchers using different techniques are briefly discussed in this section. Among all the researchers X. Q. Wang, et al¸ (2001) suggested the four components for the numerical formulation of any fluid-structure interaction problems, where the first component dealt with the modeling of the flow field around the structure which provided, the model should be versatile enough to accommodate a moving boundary in order to allow the motion of the structures, the second component is to evaluate the dynamics of the structures after the impact of flow-induced forces, the third component is the ability to resolve perfectly the fluid-structure interaction, so that, at any time the unsteady fluid forces acting on the structure can be correctly determined and the motions of the structure can be calculated at higher reliability, and finally the fourth component is the analysis of the calculated results and the calculated properties, such as velocities, lift coefficients, drag coefficients, and displacement amplitudes, etc., found to be in the time series form. The time series contains all the information concerning the behavior of the fluid flow, fluid damping and the structural dynamics. Analytical and Numerical approach for the suppression of FIV by various researchers were as follows: A. Leonard and A. Roshko., (2001) examined the numerical simulation of transversely vibrating circular cylinder in a 2-D flow. X. Gloerfelt et al., (2005), performed the analytical and numerical studies on the flow characteristics with the help of Green's and Curle's formulations. M. Lazarkov, and J. Revstedt, (2008), using a 3-D simulation (numerical formulation), analyzed the FIV oscillation of an elastically supported circular cylinder. Y. Bao et al., (2012), numerically studied the FIV characteristics of isolated and tandem elastically mounted cylinders having 2 degrees of freedom. So R.M.C. et al., (2005), carried out the numerical simulations on a long slender rigid circular cylinder in a cross-flow direction to examine three dimensional (3-D) wake effects on the flow-induced forces and also calculated and compared the results of finite volume method (FVM) with the lattice Boltzmann method (LBM). K. Yun et al, (2012), validated the numerical analysis with the extended Galerkin's method. Longatte, E., et al, suggested a fully coupled numerical approach for the numerical prediction of the vibration frequency of a flexible tube belonging to a fixed tube bundle for a fluid at rest or in flow. Q.M. Al-Mdallal et al, (2007), had done a computational study of the laminar, incompressible flow past a bluff body oscillating in the stream wise direction and it was evaluated by applying 2-D unsteady Navier–Stokes equations with nonprimitive variables. K. Schroder, H. Gelbe, (1999), carried out the simulation of FIV with the CFD (Computational Fluid Dynamics) program STAR-CD in combination with a coupled solver for the differential equations of parallel vibrating tubes for 2 and 3-dimensional calculations. Apart from that, a coupled FEM (Finite Element Method) program was used for the three-dimensional simulation of different tube support conditions. By applying a Direct Finite Difference Method, T.Tamura and E. Itoh (1997) computed the aero elastic instability of a rectangular cylinder in uniform flows and the three-dimensional unsteady flows around the oscillating cylinder with depth/breadth of 2.0 in heaving mode. D. Shiels et al, (2001), noted that the viscous vortex method was capable of achieving high resolution for the computational simulation. H. Kataoka, (2008), observed that the application of computational fluid dynamics (CFD) in wind tunnel was limited to simple problems, so it can be performed only when the inflow boundary conditions are uniform, laminar or uniformly turbulent flow. Y. Bao et al., (2011), performed the analysis for a T4/C3 MINI triangular element by applying a characteristic-based split (CBS) finite element method. T. Uchiyama, (2002), the bubbly flow around a square cylinder was forced to oscillate normally to the uniform flow, which was simulated by an incompressible two-fluid model and it was solved by applying an Arbitrary Lagrangian–Eulerian (ALE) finite element method. (Prasanth, T.K., Sanjay Mittal), carried out a stabilized finite element method in two dimensions for reduced velocity range of $2 \leq U^* \leq 15$. Gheorghe Juncu (2007), applied the vorticity–stream function formulation the Navier–Stokes equations and obtained the numerical solution in bipolar cylindrical coordinates. Sarvghad-Moghaddam Hesam et al, simulated the unsteady, viscous, incompressible and 2-D flow around two side-by-side circular cylinders using a Cartesian-staggered grid finite volume based method. Iman Harimi and Mohsen Saghafian, performed the numerical simulations with a developed finite volume code using the overset grid method. K.D. Squires et al., (2008), applied Detached-Eddy Simulation (DES) to predict the super-critical flow around the circular cylinder. L.I.R. Curling, and M.P. Paidoussis, (2003), presented the stochastic analytical equations to obtain the vibratory response of bundles of cylinders in turbulent axial flow with the various degrees of computational efficiency. Ze Li and Lixiang Zhang, (2012), solved the Navier stroke equation for the numerical simulation of 3-D unsteady turbulent flow through the flow passage of turbine model and also obtained the flow fields of flow passage along with the dynamic pressure on boundary. L. Dubcová et al, (2008), applied the stabilized finite element solution for the numerical analysis. By applying a finite-volume Total Variation Diminishing (TVD) scheme for solving the Unsteady Reynolds-Averaged Navier-Stokes (URANS) equations WANG Jia-song, (2010) studied the flows around a circular cylinder displaying an unsteady vortex shedding process at the Reynolds numbers range of 1000, 3900 and $1\times10^4$. Y. Bao et al., (2013), solved the two-dimensional incompressible Navier–Stokes equations in Arbitrary-Lagrangian–Eulerian formulation by Characteristic-Based-Split finite element method using MINI triangular element.

From the review of various researches it was observed that many researchers applied the Navier–Stokes equations, for the numerical analysis where (Baranyi, L. 2008), applied non-dimensional Navier–Stokes equations for the incompressible Newtonian fluid and expressed the equation of continuity along with the Poisson equation for pressure as follows:

$$\frac{\partial u}{\partial t} + u\frac{\partial u}{\partial x} + v\frac{\partial v}{\partial y} = -\frac{\partial p}{\partial x} = \frac{1}{\mathrm{Re}}\nabla^2 u - ao_x \quad (5)$$

$$\frac{\partial v}{\partial t}+u\frac{\partial v}{\partial x}+v\frac{\partial v}{\partial y}=-\frac{\partial p}{\partial y}=\frac{1}{\mathrm{Re}}\nabla^2 v-ao_y \quad (6)$$

$$\mathrm{D}=\frac{\partial u}{\partial x}+\frac{\partial v}{\partial y}=0 \quad (7)$$

$$\frac{\partial^2 p}{\partial x^2}+\frac{\partial^2 p}{\partial y^2}=2\left[\frac{\partial u\partial v}{\partial x\partial y}-\frac{\partial u\partial v}{\partial y\partial x}\right]-\frac{\partial D}{\partial t} \quad (8)$$

The u and v are the x and y components of the velocity, t is the time, p was the pressure, Re is Reynolds number based on the cylinder diameter d, the free-stream velocity is U, the kinematic viscosity as n, and D is the dilation. L.I.R. Curling and M.P. Paidoussis, (2003), expressed the dynamical equations governing the vibratory motions of structures in matrix form as follows:

$$\left[M(x)\frac{\partial^2}{\partial t^2}+C(x)\frac{\partial}{\partial t}+K(x)\right]\begin{Bmatrix}w(x,t)\\v(x,t)\end{Bmatrix}=\begin{Bmatrix}f_z(x,t)\\f_y(x,t)\end{Bmatrix}, \quad (9)$$

Carmo, B.S., et al., (2013), obtained the computational results by coupling the solution of the fluid flow with the solution of the structural response. The fluid flow is governed by the incompressible Navier–Stokes equations written in a non-dimensional form is expressed as:

$$\frac{\partial u}{\partial t}=-(\mathrm{u}-\mathrm{m}).\nabla u-\nabla p+\frac{1}{\mathrm{Re}}\nabla^2 u, \quad (10)$$

$$\nabla . \mathrm{U}=0,$$

The "m" was the velocity of mesh. (L.I.R. Curling, M.P. Paidoussis, 2003), expressed the Reynolds averaged equations as,

$$\nabla . \mathrm{U}=0,$$

$$\frac{\partial u_i}{\partial t}+(u.\nabla)u_i+\frac{\partial p}{\partial x_i}-\sum_{i=1}^{2}\frac{\partial}{\partial x_j}\left\{(v+v_T)\left(\frac{\partial u_i}{\partial u_j}+\frac{\partial u_j}{\partial u_i}\right)\right\}=0, \quad (11)$$

$i$ =1, 2.

Where, $v_T$ is the turbulent viscosity and it was computed on the basis of various turbulence models. Where (WANG Jia-song, 2010), expressed the governing equations for a turbulent incompressible fluid flow used in this study are the URANS with the two-equation RNG *k-ε* turbulence model.

$$\frac{\partial Q}{\partial T}+\frac{\partial F_1(Q)}{\partial X}+\frac{\partial G_1(Q)}{\partial Y}=\frac{1}{\mathrm{Re}}\left[\frac{\partial F_v(Q)}{\partial X}+\frac{\partial G_v(Q)}{\partial Y}\right]+S(Q) \quad (12)$$

**A. Arbitrary Lagrange Euler (ALE) formulation**

The Arbitrary Lagrange Euler (ALE) formulation was initially used for solving defense problem subsequently its application was extended to the free surface problems, high velocity impact, offshore structures, multi-physics problems etc. This method can also be applied for the medical applications like modeling of blood vessel deformation. Longatte, E., et al, suggests two ways to solve ALE equations: the first method is used for the study corresponding to the Eulerian viewpoint-the fully coupled equation was solved in one step; it can only handle with one-phase flow. The second method is a split method which consists of two steps to solve the ALE equations, (i) a Lagrangian step in which the mesh moves with the material velocity, and (ii) an advection step in which the mesh moves from its material position to its arbitrary position. This method was to better the model of two-phase flow-the explosion modeling for instance. Longatte, E and his colleagues numerically investigated the ALE method for evaluating the fluid-elastic parameters of a flexible tube of tube bundle for the fluid at rest or in flow. Amr Elbanhawy and Ali Turan, (2010), performed the analysis using an Arbitrary Lagrange Euler (ALE) formulation for the fluid computation.

*i. Governing equation:*

(K.Karthik Selva Kumar & L.A.Kumaraswamidhas, 2014) The aim of the computational study is to predict the vibration response of the cylinder arranged in different interference condition. Where an ALE formulation based Finite Element Method is employed to simulate the interaction of fluid flow with elastically mounted circular cylinder at different interference conditions. In turn, the ALE formulation is based on the mixed standpoint Eulerian and classical Lagrangian descriptions. The Navier–Stokes equations based on ALE formulation is written as:

$$\frac{\partial u_i}{\partial x_i}=0, \quad (12)$$

$$\rho\frac{\partial u_i}{\partial t}+\rho(u_j-\hat{u}_j)\frac{\partial u_i}{\partial x_j}=\frac{\partial \tau_{ij}}{\partial x_j}+F_i, \quad (13)$$

Where the density of the fluid is $\rho$, $u_i$ is the flow velocity, $\hat{u}_i$ is considered being the motion mesh velocity, $\tau_{ij}$ is the stress tensor, $F_i$ is force exerted from the cylinder. Apart from that, the convection velocity is replaced with relative velocity ($u_i-\hat{u}_i$) to the mesh velocity $\hat{u}_i$. The stress tensor ($\tau_{ij}$) is written as

$$\tau_{\mathrm{ij}}=-p\delta_{ij}+\mu\left(\frac{\partial u_i}{\partial x_j}+\frac{\partial u_j}{\partial x_i}\right), \quad (14)$$

in which p represents the pressure and μ represent the dynamic viscosity. In this study, the Shear Stress Transport (SST) k–$\omega$ turbulence model (Menter model) is employed for modeling the turbulence. A streamline upstream wind method, is applied to the ALE based Navier-Stokes equation with bilinear quadrilaterals for velocities and piecewise constants for pressure to obtain the finite element equations which is written as follows,

$$\mathrm{Ma}+\mathrm{N}(\mathcal{V}-\hat{\mathcal{V}})\mathcal{V}-Gp=F, \quad (15)$$

$$\mathrm{G}^t\mathcal{V}=0, \quad (16)$$

where **M** represents the mass matrix, **G** accounts for the Gradient matrix, **N** ($\mathcal{V}-\hat{\mathcal{V}}$) for the convection and viscosity, **a** for the acceleration vector, $\mathcal{V}$ represents the material velocity vector, $\hat{\mathcal{V}}$ represents the mesh velocity vector, the pressure vector is $p$, and the force vector is represented as $F$, where, M, N and G are time dependent. Whereas, at each consecutive time-step the boundary grid points are given by an analytical solution of motion equation for the structures and the inner grid points were generated by solving the Poisson equation. The software package, FLUENT, has been used to perform the flow simulations. When the flow passed the elastically mounted circular cylinder at certain velocity range, an unsteady pressure

fluctuation is acting on its surface as a result of vortex shedding, causing the bluff bodies to oscillate in the y-direction. To obtain the flow field predictions with the moving boundary of the elastically mounted cylinder, a User Defined Function (UDF) is written in C language. The objective of this UDF is to communicate with FLUENT to determine the motion of the SDOF system using the equation of motion:

$$F_y = m\frac{d^2y}{dt^2} + c\frac{dy}{dt} + ky \quad (17)$$

The UDF calculates the values of y in response to the fluid loading, at every time step. This is performed by rearranging the eqn. (16) to give the instantaneous change in velocity and the lift force coefficient $C_L$ are defined as

$$dy' = \frac{(F_y - Cy' - ky)}{m}dt \quad (18)$$

$$C_L(t) = \frac{2F_y(t)}{\rho U^2 D} \quad (19)$$

Where $F_y$ is the sum of the pressure and viscous forces on the cylinder boundary in cross flow direction; the fluid force acting upon the cylinder are computed the resulting velocity is calculated using the eqn. (18) being interpreted by FLUENT to update the vertical position of the cylinder boundary. Where, FLUENT re-meshes the computational domain in response to the new position of the boundary at each time step.

*ii. Problem description and mesh system:*

In the article, an elastically mounted circular cylinder, each of diameter D=14mm, is analyzed with different interference cylinders arranged symmetrically with respect to the Cartesian coordinates at Re=1000. The longitudinal and transverse spacing ratio between the cylinders varies from L/D=2.0,3.0,4.0 and T/D = 2.0, 3.0, 4.0 respectively. where the entire computational area is defined as $\Omega = (-20D, 50D) * (-30, 30)$. Regarding the boundary condition, a no-slip boundary condition is applied on the cylinder surface. In turn a Dirichler boundary condition is employed on the inlet is $u_1 = U_\infty \,\&\, u_2 = 0$, where at the outlet of computational area the boundary condition is $\frac{\partial u_1}{\partial x} = 0$. Whereas at the other lateral boundaries, a slip boundary condition is applied as: $\frac{\partial u_1}{\partial y} = 0 \,\&\, u_2 = 0$. To assure the mesh independency, a mesh refinement study is determined for the numerical resolution. Two cases of grid system are employed, named respectively as G1 and G2 has considered for the mesh independence study, the mesh generation parameters were shown in the table 2. At the period of mesh refinement, the time integration is performed by employing the predictor – corrector method, where the non-dimensional time integration interval is set to 0.001 for the grids G1&G2 respectively. In table 3, the global parameters of the calculated values for the elastically mounted circular cylinder are mentioned along with the percentage changes. From the table 3, is observed that the mesh changes from G1 to G2, it is evidently shows that the maximum deviation in the percentage change of 4.25% occurs in CL for the case of elastically mounted circular cylinder with two interfering cylinders arranged in staggered configuration in upstream at different spacing ratios. Bestow the test results observed, at low Reynolds number the agreeable spatial and temporal resolutions for the simulations can be obtained by employing the grid G2 at . The total mesh employed in the grid G2 for the case of an elastically mounted circular cylinder with two interfering cylinders arranged in staggered configuration in upstream at different spacing ratios consist of, total 65544 elements with 34342 nodes. The results of unsteady fluid flow over the elastically mounted circular cylinder in cross-flow direction are being used for validating the numerical accuracy.

TABLE 3. Grid independence test: A/D and $C_L$ values for the elastically mounted circular cylinder at different interference conditions: (K.Karthik Selva Kumar & L.A.Kumaraswamidhas).

| Interference condition | Grid System | Nodes on the cylinder | Elements | Nodes | A/D | $C_L$ |
|---|---|---|---|---|---|---|
| Isolated cylinder | G1 | 160 | 50162 | 25285 | 0.233 | 1.227 |
| | G2 | 200 | 54598 | 28527 | 0.225 (1.12%) | 1.235 (0.86%) |
| In tandem configuration at different spacing ratios. | G1 | 180 | 52578 | 26039 | 0.261 | 1.236 |
| | G2 | 240 | 65226 | 33065 | 0.265 (0.53%) | 1.243 (0.72%) |
| In Staggered arrangement with two interfering cylinders in downstream at different spacing Ratios | G1 | 200 | 54768 | 26894 | 0.252 | 1.331 |
| | G2 | 250 | 65431 | 34326 | 0.245 (0.78 %) | 1.373 (3.59%) |
| In staggered arrangement with two interfering cylinders in upstream at different spacing ratios | G1 | 200 | 54758 | 26886 | 0.180 | 1.310 |
| | G2 | 250 | 65544 | 34342 | 0.160 (2.46 %) | 1.363 (4.25%) |

**B. Large Eddy Simulation**

A Finite Volume Method (FVM) can be applied on the free grids along with a three dimensional incompressible unsteady Navier strokes equation, the small size eddies were solved by employing a sub-grid scale(SGS) model and the large size eddies were solved by the direct method. Besides the turbulence developed due to small scale eddies, the turbulence developed with respect to large size eddies were sturdily depends on the fluid flow geometry and its respective boundary conditions, which can be further identified through the resolved fluid flow in the LES method. In comparing to the large size eddies, the small scale eddies motions were represented by the sub-grid scale method. Further the filtering process is progressed with respect to (K.Karthik Selva Kumar & L.A.Kumaraswamidhas)

$$\bar{\phi} = \frac{1}{\Omega}\int_\Omega \phi(x')dx', \qquad x \in \Omega, . \quad (20)$$

$$G(x, x') = \begin{cases} 1/\Omega, & x' \in \Omega, \\ 0, & if not, \end{cases} \quad (21)$$

Where Ω is the volume of a computational domain, and G(x,x') is the filtering function. By applying the filtering operation, the incompressible Navier–Stokes equations for the development of the large-scale eddy motions are observed. The equations governing the Large Eddy Simulation are written as,

$$\frac{\partial \bar{u}_i}{\partial x_i} = 0, \tag{22}$$

$$\frac{\partial \bar{u}_i}{\partial t} + \frac{\partial \bar{u}_i \bar{u}_j}{\partial x_j} = \Gamma_{ij}, \tag{23}$$

$$\Gamma_{ij} = -\frac{1}{\rho}\frac{\partial \bar{p}}{\partial x_i} + \nu \frac{\partial^2 \bar{u}_i}{\partial x_j \partial x_j} - \frac{\partial \tau_{ij}}{\partial x_j}, \tag{24}$$

$$i = (1,2,3)$$

Whereas the filtered velocity components along the Cartesian coordinate's $x_i$ is represented as $\bar{u}_i$, $\bar{p}$ represent the pressure, the fluid density is represented as $\rho$ and $\nu$ represents the kinematic viscosity of the fluid. The influence of the small scales on the large (resolved) scales takes place through the sub-grid scale stress defined by

$$\tau_{ij} = \overline{u_i u_j} - \bar{u}_i \bar{u}_j \tag{25}$$

Which are remains unknown form the observed filtering operation, are being required to be modeled with a sub-grid scale model. In turn most of the sub-grid scale models were predominantly based with respect to the eddy viscosity model, which is described in the form of:

$$\tau_{ij} - \frac{1}{3}\tau_{qq}\delta_{ij} = -2\nu_t \bar{\varepsilon}_{ij}, \tag{26}$$

Further, the traces of the sub-grid scale stresses $\tau_{qq}$ is integrated with the pressure, $\nu_t$ is the kinematic viscosity of the sub-grid scale, and $\bar{\varepsilon}_{ij}$ represent the strain rate tensor for the resolved scale, Smagorinsky (1963) proposed the majority of the basic concept of sub-grid scale models which is further enhanced by Lilly (1966). In the model of Smagorinsky–Lilly, the sub-grid kinematic viscosity ( $\nu_t$ ) is derived by

$$\nu_t = l_s^2 \left|\bar{\varepsilon}_{ij}\right| \tag{27}$$

Where $l_s^2$ is the mixing length for the sub-grid scales and $\left|\bar{\varepsilon}_{ij}\right| \equiv \sqrt{2\bar{\varepsilon}_{ij}\bar{\varepsilon}_{ij}}$ .$l_s$ can be computed using

$$l_s = \min(ky, C_s \Omega^{1/3}) \tag{28}$$

Where k is the von Karman constant (k=0.41) and y is the distance to the nearest wall. *Cs* is the Smagorinsky constant, and Ω is the volume of the computational domain. Besides on that Lilly, in 1966 coined a value of Cs= 0.23 from standardized isotropic turbulence in the inertial sub range. On the other hand, this kind of higher value of the Cs is found to be resulting in an excessive damping of the high-end fluctuations in the existence of mean shear or in transitional flows, in turn small values (Cs < 0.1) may resulting in the problems with respect to convergence. From the observation of many researchers, the Smagorinsky constant (Cs = 0.1–0.14) has been found to provide better results for a wide range of flows. In the present study, all the computations were carried out by taking into consideration that the Smagorinsky constant as Cs = 0.1, besides it is acknowledged to be more appropriate value in applying Smagorinsky model for the turbulent wake simulation. (Longatte, E., et al), numerically computed the power spectral density and time record of lift and drag forces acting on tube bundles by using an unsteady fluid computation such as LES. Lam, K., et al, (2012), studied the LES for turbulent flow past two out-of-phase wavy cylinders in tandem arrangement. T. Kitagawa, H. Ohta, (2008), employed the LES with the Smagorinsky sub grid-scale model for the studies. S. Atluri et al. (2009) employed a 2-D large LES for the numerical study of the near-wake structure of a uniform flow past a circular cylinder undergoing a constant-amplitude transverse forced oscillation. K. Lam, Y.F. Lin, (2008), investigated the cross-flow around wavy cylinders of wavelength ratios k/Dm ranging from 1.136 to 3.333 using the LES.

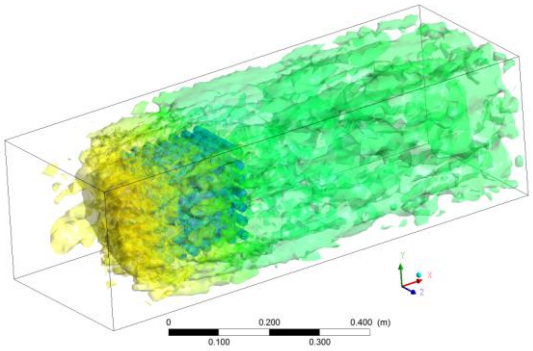


Fig 12. Iso Surface image for Multiple Cylinders at Re=1.68E4 (K.Karthik Selva Kumar & L.A.Kumaraswamidhas)

**C. Lattice Boltzmann Method (LBM)**

Lattice Boltzmann method (LBM) is an effective computational fluid dynamics (CFD) method for the fluid simulation instead of solving it through the Navier–Stokes equations. Succi, S., (2001), suggested that the LBM can be a promising numerical tool for the effective modeling of complex physics in CFD. J. Lin et al. (2013), noted that the original discrete Boltzmann's equations were based on the BGK collision term and are written as

$$f_i(X + \delta x e_i, t + \delta t) - f_i(X,t) = \frac{1}{\tau}\left[f_i(X,t) - f_i^{eq}(X,t)\right] \tag{29}$$

The motions of cylinders could be described through Newton's second law is expressed as

$$\frac{\partial^2 y_a}{\partial t^2} = \frac{2C_{La}}{\pi M^*}, \ \alpha = 1, 2. \tag{30}$$

K.Karthik Selva Kumar & L.A.Kumaraswamidhas, 2014, aimed to predict the vibration response of the side-by-side square cylinders arranged in different spacing condition. The schematic representation of elastically mounted square cylinders for the two dimensional flow simulations with the applied conditions is shown in Fig 13. In turn, the lattice-Boltzmann method (LBM) is employed in the current study to simulate the interaction of fluid flow with elastically

mounted square cylinders at three different transverse spacing ratios.

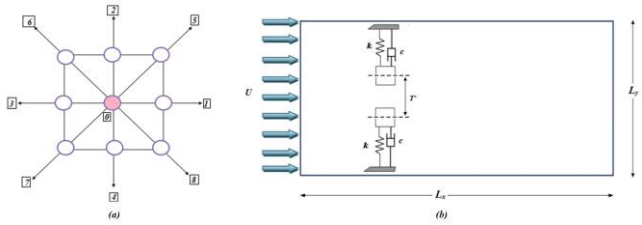

Fig 13: (a**)** Computational node with eight moving particles (representing 1-8) along with a single particle at rest (0). (b) Numerical model of elastically mounted square cylinders in cross-flow (K.Karthik Selva Kumar & L.A.Kumaraswamidhas, 2014)

In which $\vec{c}_i$ represent the unitary velocity along the direction i of a ***D'2Q9*** lattice, the ***D'*** represent the space dimensions and ***Q*** as the number of particles in the computational node adopted for the study. Where, the unitary cell is a square developed by quad, $|\vec{c}_i|$=1.0, in turn the principal direction by the quad, $|\vec{c}_i| = \sqrt{2}.0$, diagonals and by single $|\vec{c}_i| = 0$. Let $N_i(\vec{X},t)$ designates the particle dispensation in the 'i' direction of the plot $\vec{X}$ , at the time t. the Lattice Boltzmann equation with respect to Bhatnagar-Gross-Krook (BGK) collision model is written as

$$N_i(\vec{X}+\vec{c}_i,t+1)-N_i(\vec{X},t)=\frac{N_i{}^{eq}(\vec{X},t)-N_i(\vec{X},t)}{\tau}, \quad (31)$$

Where the relaxation time related to fluid kinematics viscosity is represented as $\tau$ and the $N_i^{eq}(\vec{X},t)$ is an equilibrium distribution that can be contemplate as a D2Q9 Gaussian quadrature of Maxwell-Boltzmann continuous distribution function [X. He, L.S. Luo] is given as

$$N_i^{eq}(\vec{X},t)=w_i\rho\left\{1+\frac{c_i.u}{c_s^2}+\frac{(c_i.u)^2}{2c_s^4}-\frac{u^2}{2c_s^2}\right\}, \quad (32)$$

Where $w_i$ =1/9 of the principal axis particle, i=1,2,3,4; $w_i$ =1/36 of the diagonals particles, i=5,6,7,8; and $w_0$ =4/9 for the rest of the particle respectively. For the D2Q9 lattice $c_s^2 = (1/\sqrt{3})^2$ is the square for the LB sound velocity. In each time step, the velocity flow field $\vec{u}(\vec{X},t)$ and the pressure $\vec{P}(\vec{X},t)$ respectively are deliberated by employing

$$\rho\vec{u}=\sum_i N_i\vec{c}_{i,} \quad (33)$$

$$P=c_s^2\sum_i N_i=c_s^2\rho \quad (34)$$

In order to extending the results upto an infinite number of cylinders, in this case a recurrent boundary condition is applied on the lateral sides of the cylinders (fig 1). A bounce–back condition is employed for simulating the flow adherence at the boundaries of the solids, in which, by necessitate that $N_i(X_b,t+1)=N_{-i}(\vec{X}_b,t)$ for all the b-area at the fluid domain closest to the solid-boundaries also for all the domain in the direction 'i'. Where a rough surface developed with respect to the discreteness of the considered discrete circles, which needed to enlarge the simulation domain until the results observed from simulation become insentient to the effects of discreteness. To overcome the stability related problems occurring in other methods during the simulation, as per the X. He, L.S. Luo demonstration, Lattice Boltzmann equation is considered to be a special form of discrete Boltzmann continuous equation. According to that, some attempt has been taken in consideration for the lattice Boltzmann simulations, in re to implement the irregular lattices and/or varying the mesh size. For varying the mesh size an interpolation is required, which resulting the increase in the stability related problems. Where, the present study is restricted to uniform ***D'2Q9*** lattice. The Reynolds number is calculated by using

$$\mathrm{Re}=UD/\nu \quad (35)$$

In which D represent the cylinder diameter, where $\nu=\frac{(1/2)}{3}$ is the LB kinematic viscosity in D2Q9 lattice.

The complete force exerted by the fluid on the surface of square cylinders having the surface boundary $\Gamma$ is deliberated as,

$$\vec{F}=\sum_{\Gamma}\sum_i[N_{-i}(\vec{X}_\Gamma,t^+)+N_i(\vec{X}_\Gamma,t^-)]\vec{c}_i, \quad (36)$$

Where, by deliberating the momentum variation at each area $\vec{X}_\Gamma$ in the fluid domain adjacent to the boundary surface, taking into account of the particles $N_i(\vec{X}_\Gamma,t^-)$ in the direction of 'i' indicating the surface, prior to the propagation, which were bounce back in the '–i' direction, besides propagation, $N_{-i}(\vec{X}_\Gamma,t^+)$. In turn, in this case the drag and the lift forces are in x and y direction with respect to $\vec{F}$ , where the flow pattern is proportional with respect to main flow (x) direction, the lift force is found to be zero. Normally, it is happened with respect to the immersed cylinders at smaller Reynolds number. Whenever Reynolds number increased, the vortex shedding behind the bluff bodies producing an oscillating lift and amplitude similar to the frequency of the vortices developed, the average Drag $C_d$ and Lift coefficient $C_l$ is deliberated with respect the time average as

$$C_d(t)=\frac{F(t)}{(1/2)\rho U^2 D} \quad (37)$$

$$C_l(t)=\frac{F(t)}{(1/2)\rho U^2 D} \quad (38)$$

The code employed in this study is validated by comparing the results of single square cylinder with results of previous studies. By employing a parabolic velocity inlet profile the variation in St with respect to the Re is plotted in the fig.14

$$St=fD/U \quad (39)$$

Where $f$ represent the vortex shedding frequency, in turn the observed results were found to be in good agreement with the results of previous studies, which shows the reliability of the code employed along with the spatial and temporal resolutions.

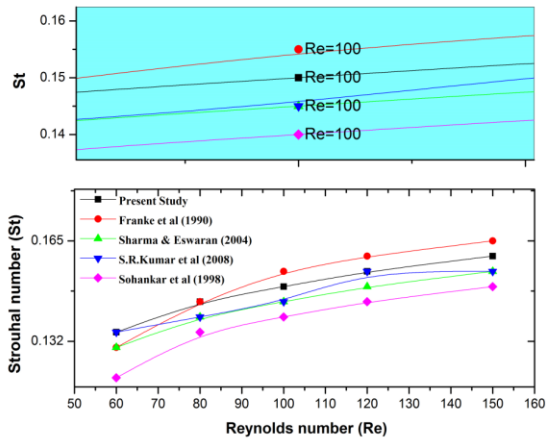


Fig. 14 Variation in the St with respect to Re for a single square cylinder, (K.Karthik Selva Kumar & L.A.Kumaraswamidhas, 2014)

The spatial ability is further tested by changing the number of respective grid points (12, 24 & 48) delineate the cylinder, also comparing the *St* values for different Re in the table 4. Regarding the 12-point grid the computational domain consist of 400 x 100 points along the longitudinal and transverse directions, gaining a blockage ratio of 0.16. where it is apparent that the difference in the St between the three resolution for a range of Re is found to be less(<5%) and further the drag coefficient and vibration amplitude indicating a difference of 2.2% and 0.5%, respectively between the grid points of 24 and 48. From the result, it is observed that at the convergence has taken place at the grid having 24points. Ensuing test with square cylinders in the cross flow satisfied with the observed results. Initially, it was identified that the variation in the results between the 12 and 24 grid point is found to be small, which suggests that the 24 grid point might be suitable for the computation. Where, the maximum value observed for the normalized *u'* (longitudinal velocity component) and *v*'(transverse velocity component, in the flip flop regime of.25% and 36% for the 12 points grid, in turn for the 24 grid point the flip flop regime is observed to be 26% and 37%.

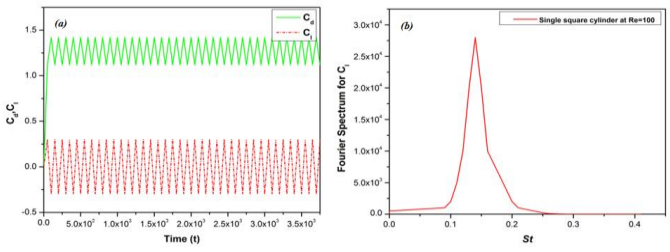


Fig. 15 (a) Cd, Cl of an elastically mounted square cylinder at Re=100; (b) Fourier spectrum of Cl at Re=100 (K.Karthik Selva Kumar & L.A.Kumaraswamidhas, 2014)

TABLE 4 Variation in the Strouhal number at different Re due to the influence of spatial resolution for a single square cylinder (K.Karthik Selva Kumar & L.A.Kumaraswamidhas, 2014)

| Reynolds number | *St* | | |
|---|---|---|---|
| | 12 points | 24 points | 48 points |
| **150** | 0.155(0.5%) | 0.157(0.5%) | 0.157 |
| **120** | 0.151(0.6%) | 0.152(0.6%) | 0.152 |
| **100** | 0.145(0.6%) | 0.146(0.5%) | 0.146 |
| **80** | 0.139(0.6%) | 0.141(0.5%) | 0.141 |
| **60** | 0.133(0.6%) | 0.135(0.6%) | 0.136 |

Besides, the test on lift and drag coefficient shows a converged result within 2%. Certainly upon increasing the resolution to 48 grid points for all the phenomena discussed in this article shows an excellent agreement with the observed value of *St*. from the above test results, the ability of producing better results on a 24 grid point is proved for all the ensuing computations.

TABLE 5 Variation in the Drag and Lift coefficient at Re = 100 due to the influence of spatial resolution for a single square cylinder (K.Karthik Selva Kumar & L.A.Kumaraswamidhas, 2014)

| | 12 points | 24 points |
|---|---|---|
| $C_d$ | 1.377(1.2%) | 1.383 |
| $C_l$ | 0.381(1.0%) | 0.386 |

## Summary & Conclusion

K.Karthik Selva Kumar & L.A.Kumaraswamidhas (2015), experimentally investigated flow induced vibration excitation response of elastically mounted circular cylinder, the following results have been observed in the course of this study. The vibration excitation at the higher cylinder frequency (30 Hz ($=5/4\,f_s$)) has no significant importance due to the stiffness of the test cylinder. Higher inconsistence in the natural frequency reduces the vibration excitation in the test cylinder because of the lack of resonance among the adjacent. Apart from that, the power spectrum shows that the vibration excitation of the test cylinder due to the induced flow of fluid observed initially at its natural frequency in the region of the beginning of the fluid elastic instability. As the velocity of the fluid is increased, the vibration in the test cylinder is observed with respect to its frequency and the frequencies of the adjacent cylinders through the fluid flow combination. When the test cylinder and the adjacent cylinders having similar natural frequency ( $f_n = f_s$ ), which results in the extremely structured oscillatory motion of the test cylinder is observed. Which were evidently proved by the principal spectra with spectral peaks in the harmonics of $f_n$ and $f_s$.

Further, a two dimensional numerically analysis is performed under with and without interference condition by arranging the cylinders in downstream and upstream

respectively, for investigating the flow induced vibration excitation response of an elastically mounted circular cylinder, the following results have been observed in the course of this study: The vibration response of the single cylinder in without interference condition, the result observed in the numerical analysis (i.e.) Maximum amplitude ratio A/D = 0.225 at reduced velocity of 5.72, is found to be almost equal to the experimental result of Maximum amplitude ratio A/D = 0.27 at reduced velocity as 6.0 respectively. Where the lock-in regime ($4.5 \leq V_r \leq 9.0$) also matches with the experimental work ($5 \leq V_r \leq 8.5$). The vibration response of the test cylinder in tandem arrangement is found to be very high when the interfering cylinder is placed in the downstream close to the test cylinder. Also, the observed amplitude ratio (A/D = 0.265) is higher than that of the isolated cylinder (A/D=0.225). In turn, the vibration excitation of the test cylinder has been reduced, when the interfering cylinder is placed further away. Among all the cylinder arrangements, the response of the cylinder in staggered arrangement with two interfering cylinders in upstream at L/D = 4.0 and T/D=2.0 spacing ratios, the oscillatory amplitude ratio is found to be minimum of A/D=0.160 at the lock-in regime of $8.5 \leq V_r \leq 21.5$ respectively. In turn, the observed result is compared with the previous studies that show that the vibration of the test cylinder is almost suppressed when the interfering cylinders placed in the upstream are very close for the same longitudinal pitch adopted as in the case of interfering cylinders placed in the downstream. However, the non-dimensional vibration frequency is observer to be nearer to 1. The response of the test cylinder with interference cylinders arranged in staggered configuration is more remarkable when the interfering cylinders are placed at the upstream of the test cylinder than the interference cylinders at downstream. However, the vibration of the test cylinder is magnified when the interfering cylinders placed at the downstream is very close. The lock-in regime is observed to be larger when the interfering cylinders are located at the upstream than the interfering cylinders that are in the downstream for same longitudinal and transverse pitch.

The following results have been observed in the course of this study by employing Lattice Boltzmann Method in square cylinders K.Karthik Selva Kumar & L.A.Kumaraswamidhas (2014). There were four different fluid flow patterns are observed at three different spacing ratios. In which a flip flop regime is observed for T/D =1.0, whereas a wiggling/Flutter shielding pattern is observed at T/D=3.5 and a synchronized flow pattern is observed for the spacing ratio of T/D=4.5. Besides that the frequencies observed for the smaller spacing ratios (T/D=1.0;3.5) having numerous peaks in the spectra. Subsequently the frequencies observed at T/D = 4.5 having a single dominating peak frequency. Besides it is identified that the main reasons for the significant variation in flow patterns is due to the changes in mean drag coefficients, root mean square values of the aerodynamic coefficients and Strouhal number. Apart from that, it is perceptible that the formation of vortex is strongly depends on the spacing ratios between the cylinders. From the results, it is identified that the cylinders at higher spacing ratios (T/D=4.5) producing minimum oscillation when compared to the smaller spacing ratios.

**SUPPRESSION OF FLOW INDUCED VIBRATION**

The important issues that must be taken into the consideration for the suppression of FIV in the bluff bodies are,

- The FIV mainly depends upon the angle of the bluff bodies arranged in the test section so it was suggested that if the bluff bodies were placed at the angle $\theta = 20° - 30°$ the vibrations on both cylinders are nearly suppressed for all regimes.
- It is possible to suppress both the structural vibration and the wake vortex on the bluff bodies by introducing a perturbation input at a high-frequency range, well-exceeding the resonant frequency of structure.
- By introducing a suitable wavy cylinder in tube bundles, it results in the suppression of flow-induced vibration of the tube bundles.
- Attaching the tripping wires in the leading stagnation line of the bluff bodies can suppress the vibration.
- Better prediction of VIV would hopefully lead to a better suppression of vibration.
- From the studies it was found that the helical strakes can be used successfully in wind engineering to suppress the VIV in chimneys and other slender structures.
- Introduction of fins was found to reduce the strength of vortex shedding slightly, in turn strongly reducing the radiated sound before the onset and during the lock-in range of the acoustic resonance.


## Acknowledgement:

Authors gratefully acknowledge the support of research grant (No.SB/FTP/ETA-389/2012) awarded by the Department of Science and Technology (DST), India.


## Nomenclateure

AR aspect (slenderness) ratio
$C_D$ mean drag force coefficient
$C_D'$ fluctuating drag force coefficient
$C_L$ mean lift force coefficient
$C_L'$ fluctuating lift force coefficient
$C_P$ mean pressure coefficient
$C_P'$ Fluctuating pressure coefficient
$C_{PB}$ Mean base pressure coefficient
$D$ Cylinder diameter (m)
$f$ Vortex shedding frequency (Hz)
$G$ Griffin number
$G$ Gap width (m)
$H$ Cylinder height, span, or length (m)
L Centre-to-Centre longitudinal spacing (pitch)
$L/D$ Longitudinal pitch ratio
$P$ Centre-to-Centre spacing (pitch) (m)
$P/D$ Pitch ratio
Re Reynolds number
St Strouhal number
$K_s$ Scruton number: mass damping parameter (2md/rB2)
$T$ Centre-to-Centre transverse spacing (pitch) (m)
$T/D$ Transverse pitch ratio
$U$ free stream velocity (m/s)
$X$ stream wise coordinates (m)
$y$ cross-stream coordinate (m)

| | |
|---|---|
| $z$ | vertical coordinate (m) |
| $\alpha$ | Incidence angle (deg) |
| $\mu$ | dynamic viscosity (Pa s) |
| $\rho$ | density (kg/m$^3$) |
| $\varphi$ | phase |
| $\mu$ | Dynamic viscosity |
| $\nu$ | Kinematic viscosity |
| $\rho$ | Density |
| $\zeta$ | Damping Parameters |
| $\zeta_s$ | Structural Damping |

## Reference:


1. Ajith Kumar, R., Gowda, B.H.L., Flow-induced vibration of a square cylinder without and with interference, Journal of Fluids and Structures, Volume 22, 345–369, 2006.
2. Ajith Kumar, R., Sugumaran, V., Gowda, B.H.L., Sohn, C.H., Decision tree: A very useful tool in analyzing flow-induced vibration data, Mechanical Systems and Signal Processing Volume 22, 202–216, 2008.
3. Aditya Kumar Pandey, Kumaraswamidhas, L.A., Kathirvelu, C., Analysis Of Flow Induced Vibration In Super heater Tube Bundles In Utility Boilers Using Computational Method, International Journal Of Computational Engineering Research / ISSN: 2250–3005, 2012.
4. Al-Mdallal, Q.M., Lawrence, K.P., Kocabiyik, S., Forced streamwise oscillations of a circular cylinder: Locked-on modes and resulting fluid forces, Journal of Fluids and Structures Volume 23, 681–701, 2007.
5. Amr Elbanhawy, Ali Turan, On Two-dimensional Predictions of Turbulent Cross-flow Induced Vibration: Forces on a Cylinder and Wake Interaction, Flow Turbulence Combust Volume 85, 199–224, 2010.
6. Assi, G.R.S., Bearman, P.W., Kitney, N., Tognarelli, M.A., Suppression of wake-induced vibration of tandem cylinders with free-to-rotate control plates, Journal of Fluids and Structures Volume 26, 1045–1057, 2010.
7. Assi, G.R.S., Meneghini, J.R.., Aranha, J.A.P., Bearman, P.W., Experimental investigation of flow-induced vibration interference between two circular cylinders, Journal of Fluids and Structures Volume 22, 819–827, 2006.
8. Atsushi Okajima, Satoru Yasui, Takahiro Kiwata, Shigeo Kimura, Flow-induced stream wise oscillation of two circular cylinders in tandem arrangement, International Journal of Heat and Fluid Flow Volume 28, 552–560, 2007.
9. Atluri,S., Rao,V.K., Dalton, C., A numerical investigation of the near-wake structure in the variable frequency forced oscillation of a circular cylinder, Journal of Fluids and Structures Volume 25, 229–244. 2009.
10. Ali Vakil, Green, Sheldon I., Two-dimensional side-by-side circular cylinders at moderate Reynolds numbers, Computers & Fluids Volume 51, 136–144. 2011.
11. Biswas, Saroj K., Ahmed, N. U.,. Optimal Control of Flow-Induced Vibration of Pipeline, Dynamics and Control, Volume 11, 187–201. 2001
12. Belvin, R.D, Flow –Induced Vibration, second ed. Van Nostrand Reinhold, New York. 1990.
13. Bhattacharyya, S., Dhinakaran, S., Vortex shedding in shear flow past tandem square cylinders in the vicinity of a plane wall, Journal of Fluids and Structures Volume 24, 400–417, 2008.
14. Berrone, S., Garbero, V., Marro, M., Numerical simulation of low-Reynolds number flows past rectangular cylinders based on adaptive finite element and finite volume methods, Computers & Fluids Volume 40, 92–112, 2011.
15. Bruno S. Carmo., Gustavo R.S. Assi., Julio R. Meneghini, Computational simulation of the flow-induced vibration of a circular cylinder subjected to wake interference, Journal of Fluids and Structures Volume 41, Pages 99–108 2013.
16. Cheng, L., Zhou, Y., Surface perturbation technique for flow-induced vibration and noise control, Journal of Sound and Vibration Volume 310, 527–540, 2008.
17. Curling, Ll.R., Paidoussis, M.P., Analyses for random flow-induced vibration of cylindrical structures subjected to turbulent axial flow, Journal of Sound and Vibration Volume 264, 795–833, 2003.
18. Delong Zuo and Nicholas P. Jones, Wind tunnel testing of yawed and inclined circular cylinders in the context of field observations of stay-cable vibrations, J. Wind Eng. Ind. Aerodyn. Volume 97, 219–227, 2009..
19. Dong, S., Karniadakis, G.E., DNS of flow past a stationary and oscillating cylinder at Re = 10 000, Journal of Fluids and Structures Volume 20, 519–531, 2005.
20. Deng.J, Ren, A.L., Shao, X.M., The flow between a stationary cylinder and a downstream elastic cylinder in cruciform arrangement, Journal of Fluids and Structures Volume 23, 715–731, 2007.
21. Eid, M., Ziada, S., Vortex shedding and acoustic resonance of single and tandem finned cylinders, Journal of Fluids and Structures Volume 27, 1035–1048, 2011.
22. Fenghao WANG., Gedong JIANG., John Zhang Lin., Simulation of cross-flow-induced vibration of tube bundle by surface vorticity method, Front. Energy Power Eng. China Volume 2(3): 243–248. 2008.
23. Fleck, B.A., 2001. Strouhal numbers for flow past a combined circular–rectangular prism, Journal of Wind Engineering and Industrial Aerodynamics Volume 89, 751–755.
24. Franzini, G.R., Fujarra, A.L.C., Meneghini, J.R., Korkischko, I., Franciss, R., Experimental investigation of Vortex-Induced Vibration on rigid, smooth and inclined cylinders, Journal of Fluids and Structures Volume 25, 742–750. 2009.
25. Gunter Schewe, Reynolds-number-effects in flow around a rectangular cylinder with aspect ratio 1:5, Journal of Fluids and Structures, Volume 39, 15–26, 2013,
26. Gheorghe Juncu, A numerical study of momentum and forced convection heat transfer around two tandem circular cylinders at low Reynolds numbers.

Part I: Momentum transfer, International Journal of Heat and Mass Transfer Volume 50, 3788–3798, 2007.
27. Gabbai, R.D., Benaroya, H., An overview of modeling and experiments of vortex-induced vibration of circular cylinders, Journal of Sound and Vibration,Volume 282, 575–616, 2005.
28. Gloerfelt, X., Perot, F., Bailly, C., Juve, D., Flow-induced cylinder noise formulated as a diffraction problem for low Mach numbers, Journal of Sound and Vibration, Volume 287, 129–151, 2005.
29. Gelbe, H., Jahr, M., Schroder, K., Flow-induced vibrations in heat exchanger tube bundles, Chemical Engineering and Processing, Volume 34, 289-298, 1995.
30. Hiroto Kataoka,. Numerical simulations of a wind-induced vibrating square cylinder within turbulent boundary layer, Journal of Wind Engineering and Industrial Aerodynamics, Volume 96, 1985–1997. 2008.
31. Huera-Huarte, F.J., Gharib, M., Flow-induced vibrations of a side-by-side arrangement of two flexible circular cylinders, Journal of Fluids and Structures, Volume 27, 354–366. 2011.
32. Hemon, P., Santi, F., Schnoerringer, B., Wojciechowski, J., Influence of free-stream turbulence on the movement-induced vibrations of an elongated rectangular cylinder in cross-flow, Journal of Wind Engineering and Industrial Aerodynamics, Volume 89, 1383–1395. 2001.
33. Hyun-Boo Lee, Tae-Rin Lee, Yoon-Suk Chang, "Numerical simulation of flow-induced bi-directional oscillations" Journal of Fluids and Structures, Volume 37, Pages 220–231, 2013.
34. In-Cheol Chu, Heung June Chung, Seungtae Lee, Flow-induced vibration of nuclear steam generator U-tubes in two-phase flow, Nuclear Engineering and Design, Volume 241, 1508–1515, 2011.
35. Iman Harimi., Mohsen Saghafian., Numerical simulation of fluid flow and forced convection heat transfer from tandem circular cylinders using overset grid method, Journal of Fluids and Structures, Volume 28, 309–327, 2012.
36. Ian Taylor, Marco Vezza, Calculation of the flow field around a square section cylinder undergoing forced transverse oscillations using a discrete vortex method, Journal of Wind Engineering and Industrial Aerodynamics, Volume 82, 271-291, 1999.
37. Jubran, B. A., Hamdan, M. N., Shabaneh, N. H., Wavelet and chaos analysis of flow induced vibration of a single cylinder in cross- flow, International Journal of Engineering Science, Volume 36, 843±864, 1998.
38. Jeon, D. and Gharib, M., On circular cylinders undergoing Two-degree-of-freedom forced motions, Journal of Fluids and Structures, Volume 15, 533-541, 2011.
39. Jin, W., Zhou, Y., Chan, P.K.C., Xu, H.G., A fibre-optic grating sensor for the study of flow-induced vibrations, Sensors and Actuators, Volume 79, 36–45, 2000.
40. Joly, A., Etienne, S., Pelletier, D., Galloping of square cylinders in cross-flow at low Reynolds numbers, Journal of Fluids and Structures, Volume 28, 232–243, 2012.
41. Jianzhong Lin., Renjie Jiang., Zhongli Chen., Xiaoke Ku., Poiseuille flow-induced vibrations of two cylinders in tandem, Journal of Fluids and Structures, Volume 40, 70–85 2013.
42. Karthik Selva Kumar K., Kumaraswamidhas L. A. Experimental investigation on flow induced vibration excitation in the elastically mounted circular cylinder in cylinder arrays. Fluid Dynamic Research, 47, 015508. 2015.
43. Karthik Selva Kumar K., Kumaraswamidhas L. A. Experimental investigation on flow induced vibration excitation in the elastically mounted square cylinders. Journal of Vibroengineering,17, 468-477. 2015.
44. K.Karthik Selva Kumar, K.Aruna Devi, and L.A. Kumaraswamidhas, SPSS: A Data mining tool for analyzing the results of flow induced vibration excitation in an elastically mounted circular cylinder at different interference conditions, Applied Mechanics and Materials, 592-594, 2086-2090. 2014.
45. K.Karthik Selva Kumar, L.A. Kumaraswamidhas, Numerical Study on Fluid Flow Characteristics Over the Side-By-Side Square Cylinders at Different Spacing Ratio, International Review of Mechanical Engineering, 2014, 8, 962-969. 2014.
46. K.Karthik Selva Kumar, L.A. Kumaraswamidhas, A Study on Flow Induced Vibration Excitation in Solid Square Structures", International Journal of Mechanical & Production Engineering Research and Development, 4(4), 15-22. 2014.
47. Korkischko, I., Meneghini, J.R., Experimental investigation of flow-induced vibration on isolated and tandem circular cylinders fitted with strakes. Journal of Fluids and Structures, Volume 26, 611–625. 2010.
48. Kenan Yakut., Bayram Sahin., Suat Canbazoglu, Performance and flow-induced vibration characteristics for conical-ring turbulators, journal of Applied Energy, Volume 79, 65–76. 2004.
49. Kang, H.S., Song, K.N., Kim, H.K., Yoon, K.H., Axial-flow-induced vibration for a rod supported by translational springs at both ends, Nuclear Engineering and Design, Volume 220, 83-90. 2003.
50. KimVandiver, J.,. Damping Parameters for flow-induced vibration, Journal of Fluids and Structures, Volume 35, 105–119, 2012
51. Kyungjae Yun., Jongwoon Choi., Sung-Kyun Kim., Ohseop Song, Flow-induced vibration and stability analysis of multi-wall carbon nanotubes, Journal of Mechanical Science and Technology, Volume 26 (12), 3911-3920. 2012.
52. Kitagawa, T., Fujino, Y., Kimura, K., Mizuno, Y.,. Wind pressures measurement on end-cell-induced vibration of a cantilevered circular cylinder, Journal of Wind Engineering and Industrial Aerodynamics, Volume 90, 395–405. 2002.
53. Kitagawa, T., Ohta, H., Numerical investigation on flow around circular cylinders in tandem arrangement at a subcritical Reynolds number, Journal of Fluids and Structures, Volume 24, 680–699. 2008.
54. Lam, K., Lin, Y.F., Zou, L., Liu, Y., Experimental study and large eddy simulation of turbulent flow around tube bundles composed of wavy and circular

cylinders International Journal of Heat and Fluid Flow, Volume 31, 32–44. 2010.
55. Longatte, E., Bendjeddou, Z., Souli, M., Methods for numerical study of tube bundle vibrations in cross-flows, Journal of Fluids and Structures, Volume 18, 513–528. 2003.
56. Lam, K., Lin, Y.F., Zou, L., Liu, Y., Numerical simulation of flows around two unyawed and yawed wavy cylinders in tandem arrangement, Journal of Fluids and Structures, Volume 28, 135–151, 2012.
57. Lam, K., Li, J.Y., Chan, K.T., So, R.M.C., Flow pattern and velocity field distribution of cross-flow around four cylinders in a square configuration at a low Reynolds number, Journal of Fluids and Structures, Volume 17, 665–679, 2003.
58. Luo, S.C., Tan, Roy X.Y., Induced parallel vortex shedding from a circular cylinder at Re of O ($10^4$) by using the cylinder end suction technique, Experimental Thermal and Fluid Science, Volume 33, 1172–1179, 2009.
59. Lixia Qu., Christoffer Norberg., Lars Davidson., Shia-Hui Peng., Fujun Wang., Quantitative numerical analysis of flow past a circular cylinder at Reynolds number between 50 and 200, Journal of Fluids and Structures, Volume 39, May 347-370, 2013.
60. Lenka Dubcova., Miloslav Feistauer., Jaroslav Horacek., Petr Svacek., Numerical simulation of airfoil vibrations induced by turbulent flow, Journal of Computational and Applied Mathematics, Volume 218, 34 – 42, 2008.
61. Leonard, A., Roshko, A., Aspects of Flow-Induced Vibration, Journal of Fluids and Structures, Volume 15, 415 – 425, 2001.
62. Lazarkov, M., Revstedt, J., Flow-induced motion of a short circular cylinder spanning a rectangular channel, Journal of Fluids and Structures, Volume 24, 449–466. 2008.
63. Lau, Y.L., So, R.M.C., Leung, R.C.K., Flow-induced vibration of elastic slender structures in a cylinder wake, Journal of Fluids and Structures, Volume 19, 1061–1083, 2004.
64. Lam, K., Li, J.Y., So, R.M.C., Force coefficients and Strouhal numbers of four cylinders in cross flow, Journal of Fluids and Structures, Volume 18, 305–324, 2003.
65. Lam, K., Lin, Y.F., Large eddy simulation of flow around wavy cylinders at a Subcritical Reynolds number, International Journal of Heat and Fluid Flow, Volume 29, 1071–1088. 2008.
66. Ming Zhao., Numerical investigation of two-degree-of-freedom vortex-induced vibration of a circular cylinder in oscillatory flow, Journal of Fluids and Structures, Volume 39, 41-59 2013.
67. Meneghini, J.R., Saltara, F., Siqueira, C.L.R., Ferrari JR, J.A., Numerical Simulation of Flow Interference Between two Circular cylinders in tandem and Side-by-side Arrangements, Journal of Fluids and Structures, Volume 15, 327-350. 2001.
68. Mohany, A., Ziada, S., Flow-excited acoustic resonance of two tandem cylinders in cross-flow, Journal of Fluids and Structures, Volume 21, 103–119. 2005.
69. Muk Chen Ong., Torbjørn Utnes., Lars Erik Holmedal., Dag Myrhaug., Bjørnar Pettersen., Numerical simulation of flow around a smooth circular cylinder at very high Reynolds numbers, Marine Structures, Volume 22, 142–153, 2009.
70. Mahbub Alam, Md., Zhou, Y., Strouhal numbers, forces and flow structures around two tandem cylinders of different diameters, Journal of Fluids and Structures, Volume 24, 505–526. 2008.
71. Muammer Ozgoren., Engin Pinar., Besir Sahin., Huseyin Akilli., Comparison of flow structures in the downstream region of a cylinder and sphere, International Journal of Heat and Fluid Flow, Volume 32, 1138–1146. 2011.
72. Mahbub Alam, Md., Sakamoto, H., Zhou, Y., Determination of flow configurations and fluid forces acting on two staggered circular cylinders of equal diameter in cross-flow, Journal of Fluids and Structures, Volume 21, 363–394. 2005.
73. Mittal, S., Kumar, V., Flow-Induced Vibrations of a Light Circular Cylinder at Reynolds Numbers $10^3$ to $10^4$, Journal of Sound and Vibration, Volume 245(5), 923-946. 2001.
74. Mittal, S., Kumar, V., Flow-induced oscillations of two cylinders in tandem and staggered arrangements, Journal of Fluids and Structures, Volume 15, 717 – 736, 2001.
75. Matsuda, K., Uejima, H., Sugimoto, T., Wind tunnel tests on in-line oscillation of a two-dimensional circular cylinder, Journal of Wind Engineering and Industrial Aerodynamics, Volume 91, 83–90. 2003.
76. Norberg, C.,. Fluctuating lift on a circular cylinder: review and New measurements, Journal of Fluids and Structures, Volume 17, 57–96. 2003.
77. Okajima, A., Nagamori, T., Matsunaga, F., Kiwata, T., Some Experiments on flow-induced Vibration of a circular cylinder with Surface roughness, Journal of Fluids and Structures, Volume 13, 853-864. 1999.
78. Paidoussis, M.P., Real-life experiences with flow-induced vibration, Journal of Fluids and Structures, Volume 22, 741–755. 2006.
79. Perotin, L., Granger, S., An Inverse Method For The Identification Of A Distributed Random Excitation Acting On A Vibrating Structure Part 2: Flow-Induced Vibration Application, Mechanical Systems and Signal Processing, Volume 13 (1), 67-81. 1999.
80. Prasanth, T.K., Sanjay Mittal., Vortex-induced vibration of two circular cylinders at low Reynolds number, Journal of Fluids and Structures, Volume 25, 731–741. 2009.
81. Pettigrew, M.J., Taylor, C.E., Fisher, N.J., Yetisir, M., W. Smith B.A. Flow-induced vibration: recent findings and open questions, Nuclear Engineering and Design, Volume 185, 249±276. 1998.
82. Pasto, S., Vortex-induced vibrations of a circular cylinder in laminar and turbulent flows, Journal of Fluids and Structures, Volume 24, 977–993. 2008.
83. Raghavan, K., Bernitsas, M.M., Experimental investigation of Reynolds number effect on vortex induced vibration of rigid circular cylinder on elastic

supports, Ocean Engineering, Volume 38, 719–731. 2011.
84. Ryan, K., Pregnalato, C.J., Thompson, M.C., Hourigan, K., Flow-induced vibrations of a tethered circular cylinder, Journal of Fluids and Structures, Volume 19, 1085–1102. 2004.
85. Rojratsirikul, P., Genc, M.S., Wang, Z., Gursul, I, Flow-induced vibrations of low aspect ratio rectangular membrane wings, Journal of Fluids and Structures, Volume 27, 1296–1309. 2011.
86. So, R.M.C., Liu, Y., Cui, Z.X., Zhang, C.H., Wang, X.Q., Three-dimensional wake effects on flow-induced forces, Journal of Fluids and Structures, Volume 20, 373–402. 2005.
87. Schroder, K., Gelbe, H., Two- and three-dimensional CFD-simulation of flow-induced vibration excitation in tube bundles, Chemical Engineering and Processing, Volume 38, 621–629. 1999.
88. Sang-Nyung Kim, Yeon-Sik Cho, The Analysis of Flow-Induced Vibration and Design Improvement in KSNP Steam Generators of UCN #5, 6, KSME International Journal, Volume 18(1), 74 - 81. 2004.
89. So, R.M.C., Liu, Y., Lai, Y.G., Mesh shape preservation for flow-induced vibration problems, Journal of Fluids and Structures, Volume 18, 287–304. 2003.
90. Sumner, D., Two circular cylinders in cross-flow: A review, Journal of Fluids and Structures, Volume 26, 849–899. 2010.
91. Shiels, D., Leonard, A., Roshko, A., Flow-Induced Vibration of a Circular Cylinder at Limiting Structural Parameters, Journal of Fluids and Structures, Volume15, 3-21. 2001.
92. Sumner, D., Richards, M.D., Akosile, O.O., Two staggered circular cylinders of equal diameter in cross-flow, Journal of Fluids and Structures, Volume 20, 255–276. 2005.
93. Squires, Kyle D., Vivek Krishnan., Forsythe, James R., Prediction of the flow over a circular cylinder at high Reynolds number using detached-eddy simulation, Journal of Wind Engineering and Industrial Aerodynamics, Volume 96, 1528–1536. 2008.
94. Sarvghad-Moghaddam Hesam, Nooredin Navid., Ghadiri-Dehkordi Behzad, Numerical simulation of flow over two side-by-side Circular cylinders, Journal of hydrodynamics, Volume 23(6), 792-805. 2011.
95. Satoshi Someya., Joji Kuwabara., YanRong Li., Koji Okamoto., Experimental investigation of a flow-induced oscillating cylinder with two degrees-of-freedom, Nuclear Engineering and Design, Volume 240, 4001–4007, 2010.
96. Tamura, T., Itoh, Y., Three-dimensional vortical flows around a bluff cylinder in unstable oscillations, Journal of Wind Engineering and Industrial Aerodynamics, Volume 67&68, 141-154, 1997.
97. To, A.P., Lam, K.M., Flow-induced vibration of a flexibly mounted circular cylinder in the proximity of a larger cylinder downstream, Journal of Fluids and Structures, Volume 23, 523–528. 2007.
98. Tomomi Uchiyama, Finite element analysis of bubbly flow around an oscillating square-section cylinder, Finite Elements in Analysis and Design, Volume 38, 803–821. 2002.
99. Takayuki Tsutsui., Experimental study on the instantaneous fluid force acting on two circular cylinders closely arranged in tandem, Journal of Wind Engineering and Industrial Aerodynamics, Volume 109, 46–54. 2012.
100. Wang, Z.J., Zhou, Y., Vortex interactions in a two side-by-side cylinder near-wake, International Journal of Heat and Fluid Flow, Volume 26, 362–377. 2005.
101. Wolfe, D., Ziada, S., Feedback control of vortex shedding from two tandem cylinders, Journal of Fluids and Structures, Volume 17, 579–592. 2003.
102. Williamson, C.H.K., Govardhan, R., A brief review of recent results in vortex-induced vibrations, Journal of Wind Engineering and Industrial Aerodynamics, Volume 96, 713–735. 2008.
103. Wang Jia-song, Flow Around a Circular Cylinder Using a Finite-Volume TVD Scheme Based on a Vector Transformation Approach, Journal of hydrodynamics, Volume22(2), 221-228. 2010.
104. Wang, X. Q., So, R.M.C., Liu, Y., Flow-Induced Vibration of an Euler – Bernoulli Beam, Journal of Sound and Vibration, Volume 243(2), 241- 268, 2001.
105. Wu, W., Yuan, J., Cheng, L., Multi-high-frequency Perturbation effects on flow-induced vibration control, Journal of Sound and Vibration, Volume 305, 226–242. 2007.
106. Xiaodong Wu., Fei Ge., Youshi Hong, A review of recent studies on vortex-induced vibrations of long slender cylinders, Journal of Fluids and Structures, Volume 28, 292–308. 2012.
107. Yan Bao, Dai Zhou, Jiahuang Tu, Flow interference between a stationary cylinder and an elastically mounted cylinder arranged in proximity, Journal of Fluids and Structures, Volume 27, 1425–1446. 2011.
108. Yan Bao, Cheng Huang, Dai Zhou, Jiahuang Tu, Zhaolong Han, Two-degree-of-freedom flow-induced vibrations on isolated and tandem cylinders with varying natural frequency ratios, Journal of Fluids and Structures, Volume 35, 50–75. 2012.
109. Yan Bao, Dai Zhou, Jiahuang Tu, Flow characteristics of two in-phase oscillating cylinders in Side-by-side arrangement, Computers & Fluids, Volume 71, 124–145. 2013.
110. Zou, G.P., Cheraghi, N., Taheri, V., Fluid-induced vibration of composite natural gas pipelines, International Journal of Solids and Structures, Volume 42, 1253–1268. 2005.
111. Zhide XI, Bingde CHEN, Pengzhou LI, Large eddy simulation of turbulent buffet forces in flow induced vibration, Energy Power Eng. China, Volume 2(4), 524–527. 2008.
112. Ze Li., Lixiang Zhang., Research on numerical method of flow-induced vibration on spiral casing structure of large-scale hydropower station, International Conference on Advances in Computational Modeling and Simulation, Procedia Engineering, Volume 31, 688 – 695. 2012.